PNAS
www.pnas.org

Supplementary Information for

Canine olfactory detection of a vectored phytobacterial pathogen, *Candidatus* Liberibacter asiaticus, and integrated disease control

Timothy Gottwald, Gavin Poole, Thomas McCollum, David Hall, John Hartung, Jinhe Bai, Weiqi Luo, Drew Posny, Yong-Ping Duan, Earl Taylor, John da Graça, Marylou Polek, Frank Louws, William Schneider

Correspondence to: tim.gottwald@usda.gov

This PDF file includes:

Other Supplementary Materials for this manuscript include the following:

www.pnas.org/cgi/doi/10.1073/pnas.1914296117

Materials and Methods

A.

Sensitization to disease-related odor and assessment of *C*Las detection accuracy. To assess sensitivity, specificity, and other latent class statistical metrics of detection accuracy, the 10 trained canines ran the 100-tree grid in sequence. The position and number of *C*Las positive trees within grid was then re-randomized, and the 10 canines repeated running the grid in sequence until 9 dogs had run 10 replicates of the 100 tree grid for a total of 1000 assessments per canine. A 10th canine ran 5 replicates of 100 trees but was unable to complete all 10 replicates due to illness. Thus, the canines assessed $N = 9{,}500$ trees as a group. To measure the performance of canines individually and as a group, a binary classification test was performed on the data and the following latent-class metrics calculated:

True Positive (TP) correct canine alert on *C*Las-positive tree
True Negative (TN) correct rejection, no alert on *C*Las-negative tree
False Positive (FP) false alert on *C*Las-negative tree, Type I error
False Negative (FN) missed *C*Las-positive target, Type II error
Sensitivity (SEN) or true positive rate,

$$SEN = TP/(TP + FN)$$

Specificity (SPE) or True Negative Rate

$$SPE = TN/(FP + TN)$$

Precision or Positive Predictive Value (PPV)

$$PPV = TP/(TP + FP)$$

Negative Predictive Value (NPV)

$$NPV = TN/(TN + FN)$$

False Positive Rate (FPR)

$$FPR = FP/(FP + TN)$$

False Negative Rate (FNR)

$$FNR = FN/(FN + TP)$$

False Discovery Rate (FDR)

$$FDR = FP/(TP + FP)$$

Accuracy (ACC)

$$ACC = (TP + TN)/n$$

Probability (*P*)

$$P = (k!(q-k)!)/q!)^{lm}$$

Where n = total population assessed, q = number of positions in the test line or grid, k = number of test samples (ex. *C*Las positives) in the line or grid, l = number of canines used in the assay, m = the number of replications, and $!$ = the factorial of the indicated variable.

No single performance metric can capture all aspects of canine detection accuracy. Throughout this study we key on three commonly cited metrics; *sensitivity* (SEN), *specificity* (SPE) and *accuracy* (ACC). However, we calculate and present a number of performance metrics in order to allow the reader to examine and interpret canine detection accuracy from various perspectives.

For instance, PPV and NPV are informative metrics; PPV estimates the probability that a positive test result actually means the detection of the target scent when present and NPV estimates the probability that a negative test result actually means the nondetection of the target scent when not present. *P* is the probability of correct indication by chance in repeated trials with multiple canines. It is useful to note that while PPV and NPV indicate the probability of positive and negative outcomes from an inspection being, respectively, infected and uninfected, they are dependent on the prevalence of disease in the population being tested. In contrast, SEN and SPE are properties of the canine diagnostic and independent of disease prevalence.

B. Canine-handler team performance. We examined if canine *C*Las detection accuracy differed depending upon the handler with whom they were teamed or who was conducting the test replicate. The number of errors was exceedingly low across all canine detectors regardless of the canine-handler combination. However, there was a non-significant trend across all canines with more prevalent FP errors when paired with Handler 2 (Fig. 1 B,C,D).

C. Improvement of canine detection accuracy by consensus. Using latent class metrics, we examined pairing canines to determine if TP detection precision could be improved beyond the 0.9905 described above by deploying pairs of canines to interrogate the same tree(s) of unknown *C*Las status (Fig. S3). Ex post analysis of the two groups of five canines were paired in all possible combinations within each group. Of the 20 combinations examined, detection accuracy improved for all but one of the pairings in some cases to 100%. Thus depending upon the level of accuracy desired, the deployment of multiple canine detectors to interrogate the same trees is beneficial. We also determined that detection accuracy increased to 1.0000 when using a consensus of the majority 2/3 or 3/3 canines (Fig. S4).

D. Spatial heterogeneity of *C*Las detection errors. False positive alerts can be caused by the dissemination of the odor plume around an odor source. Jezierski states, *"Ideally, dogs should alert as close as possible to the site where the odorous material is hidden by comparing the differences in odor concentration inside the odor plume. It is common for a dog to enter, then exit and reenter the scent cone during odor detection which may account for number of times a canine passed a hide as demonstrated in the data. The role of the distribution of the odor plume was evident in our experiment when comparing the percentage of false alerts in particular searching sites. When searching outdoors the distribution of the odor plume may often enable a more easily directional scenting and localization of odor source, which thus takes less time with more correct and fewer false alerts*" (*52*). Craven found that the odor plume of a drug moves and disperses, depending on air currents, humidity, temperature, or features in the terrain, and may also influence the detection performance (*53*). The fluid dynamics of odorant transport during sniffing has not been extensively examined. Angle stated that *"Much more research needs to be conducted in order to understand the movement of biological VOC within the thermal plume (e.g., micro currents) and in the aerodynamic wake/wind currents in order to develop search patterns to optimize biomedical detection*" (*54*).

Thus, it is well demonstrated that canine detectors can pick up a target scent at some distance. In addition to the spatial heterogeneity experiment indicated in the main paper, we conducted a spatial assessment of the detection data to determine if proximity of *C*Las-positive trees positioned immediately adjacent to, at oblique angles to, or upwind from canine FNs or FPs were related to the cause of the error.

We examined the distance of FP alerts to prior TP locations to determine if FPs are more likely to be found near prior TP locations. However, there was insufficient FP indications within the combined trial data to draw any conclusions on distance or spatial relationships to prior TPs (Fig. S5 A,B). We also investigated for a defined spatial heterogeneity of FP errors near the perimeter of the trial plot. There was no significant spatial dependency of FP errors for distance to the nearest TP, *C*Las-infected tree, nor to all TP in the proximity. Additionally there was no significant spatial dependency to the perimeter or edge effects (Fig. S6 A-C).

E. Volatilome and VOC assay. The biochemical mechanisms underlying the release of disease-related VOC are largely unknown (*55-57*). To date no published studies define which, if any, VOCs are detectable as an odor by dogs and the identity of the specific VOCs on which dogs alert in relation to infection is speculative (*55*). Gas chromatography-Mass spectrophotometric (GC-MS) analysis demonstrated a unique composition of multiple VOCs associated with *C*Las-infected plants versus non-infected plants indicating differential volatilomes serving as nontarget versus target odor sources, respectively. Initially we thought that the *C*Las infected plant signature does not emanate from the pathogen itself, but rather is due to the bacterial elicited physiological changes in the host that gives off unique changes in volatilome scent signature in response to infection. Contemplating this hypothesis we thought it likely that infected hosts emit increases in some VOCs while depressing others, resulting in unique changes in the complex scent signature of citrus when infected by *C*Las. We later determined that this is not the case and that canines are actually detecting the *C*Las pathogen itself (see text). Even so, it is quite possible that the compliment of VOCs in the scent signature is composed of some VOC changes below the detection threshold of GC-MS.

F. Assessment of *C*Las infection via qPCR. The following qPCR primers and protocols (*13,41*) were used to determine the clinical infection status of *C*Las-inoculated and/or field trees canine studies. Two to four leaves with petioles were detached from each shoot from two or more major tree branches. DNA was extracted from the midrib/petiole of the sampled leaves. For each tree, a combined sample of 100 to 180 mg of midrib tissue was excised before DNA extraction. After extraction, total nucleic acids in each sample was quantified using a nano-drop spectrophotometer (Nanodrop 2000; Thermo Scientific, USA) and standardized to 50 ng·mL–1 with nuclease-free sterile water. The quantitative TaqMan PCR method uses 16S rDNA-based primer-probe sets specific to CLAS. The primer/probe system employed was labeled with NED/MGB, i.e., it uses a TaqMan minor groove binding probe, which incorporates a 5' reporter dye and a 3' nonflourescent quencher. The reporter dye used was NED. This system was optimal for use on the real-time PCR instrument with a FAST platform (Applied Biosystems by ThermoFisher Scientific, Carlsbad, CA). Applied Biosystems Taqman Fast Advanced Master Mix was used with the addition of the primers, probe, nuclease-free water, and polyvinylpyrrolidone

(PVP). The primers were used at a concentration of 0.3 mM, the probe at 0.15 mM, and the PVP (added to bind PCR reaction inhibitors) at 25 mg·mL–1 mix. Total volume per each of the 96 wells/plate was 20 mL. The cycle parameters of the real-time program were: 95° C for 20 s followed by 40 cycles of 95° C for 3 s and 60° C for 30 s. The instrument software (ABI software; International Trade Systems, Portland, OR) calculates a noise baseline from fluorescent background in the early cycles of the PCR reaction, whereas the signal from target amplification is negligible. A threshold value is then automatically calculated indicating a statistically significant point above the background noise and data for a sample is reported as threshold cycle (Ct) value, which is the number of PCR cycles necessary to reach significant sample signal. Lower Ct values indicate higher initial template in the well, requiring fewer amplification cycles to reach the threshold of significance. For our studies, we considered Ct values of ≤ 36 or ≤ 38.5 which reflect two regulatory Ct thresholds that have been used by USDA, APHIS over time as indicative of as positive qPCR assay for the pathogen.

G. Assessment of canine subclinical *C*Las detection. *C*Las has a prolonged incubation period of several months to years between infection and HLB symptom expression. Similarly, there is a prolonged subclinical period of weeks to years between infection and detection by qPCR depending on age, size and physiological status of an infected tree. However, it was noted that canines were capable of detecting *C*Las-positive trees during this subclinical period. A temporal study was designed to assess the point in the subclinical period at which canines can detect *C*Las-inoculated trees compared with qPCR (current default gold and regulatory standard). A group of 30 trees were inoculated by caging the terminal shoot of each tree and placing 20 presumptive *C*Las-bacterialiferous psyllids within the cage. Presumptive *C*Las-bacterialiferous psyllids were taken from a psyllid colony continuously feeding on and presumably acquiring *C*Las from *C*Las-positive trees. The inoculated trees were assessed weekly via qPCR and via the canines. For qPCR, 4-6 leaves (depending on the amount of foliage to choose from so as not to oversample and defoliate the trees) and 100-150 mg (wet) 60-100 mg (dry) root tissue/tree as described above. The experiment was completely blind during sampling because it was not possible to determine the infection status of the trees until the infections increased in bacterial populations beyond the minimal threshold for qPCR and eventually became qPCR-positive, i.e., clinically positive, often several months after the bi-weekly canine interrogation.

For this trial, 10 canines assessed a randomized mixed population of 90 non-infected and 10 presumptive *C*Las-positive trees in a 10 X 10 tree array bi-weekly for the first 25 weeks at which point agreement of *C*Las infection status was stable among the 10 canines. The assays were replicated 3 times during each assay date. Data were later combined across replications. All 30 trees were successfully detected by one or more canines in combination within the first month. However, qPCR status continued to be assayed monthly. Over the 32-mo. course of the study, 16 and 20 of the initial 30 trees inoculated via psyllids were confirmed by qPCR as *C*Las-positive at Ct ≤ 36 and 38.5, respectively, over the duration of the experiment. Additionally, to reach these optimums of *C*Las-positive detection required 16 and 17 months post inoculation at qPCR thresholds of Ct ≤36 and 38.5, respectively. Once canine detection reached an optimum at 7

months canine assays were discontinued but resumed at 30 and 32 months to demonstrate that canines as a group maintained at >90% detection over time (Figs. 3, S7, S8).

Because only a few leaves or a small amount of root tissue could be destructively sampled each assessment date, and because *C*Las infection is erratically distributed in trees, trees were not consistently qPCR clinically positive over time. The number of canines correctly identifying each *C*Las-positive tree (testing qPCR positive on one or more assessment dates) were graphed over time along with their qPCR status. The time between inoculation and canine detection (ΔT_{canine}) and the time between infection and qPCR confirmation (ΔT_{PCR}), were calculated for each of the trees that was eventually confirmed to be *C*Las-positive.

H. Assessment of *C*Las-infection from citrus root tissue. Approximately 3g of feeder root tissue was collected from *C*Las-infected trees (confirmed via qPCR) and from containment greenhouse *C*Las-free trees as a negative control. All samples were washed free of visible soil residue, maintained turgid by wrapping in moistened paper towels, and used within 2 days of harvest. Nine trained canines each interrogated a 5X5 array consisting of metal cans into which the test root tissue was placed. Two of the 25 cans were randomly selected to hold *C*Las-positive root tissue and the remainder non-infected root tissue. The cans were randomized after each of 5 replications and the test repeated once. Metal cans were used to ensure that the VOCs were contained and did not permeate the soil on which they were placed. Performance was measured by the same metrics as for the assessment of *C*Las detection accuracy described above.

I. Assessment of discrimination of *C*Las from other citrus pathogens. Four trained canines were transported to the USDA, Agricultural Research Service, Molecular Plant Pathology Laboratory and Exotic Pathogens of Citrus Collection (EPCC) in Beltsville, MD. The laboratory maintains an international *in vivo* collection of several hundred accessions of citrus pathogens from around the world. To test canine discrimination for *C*Las-infected trees versus trees infected with other pathogenic organisms, a 20-tree grid (2 rows of 10 trees ~3 m apart within and across row) of mixed non-infected and potential target (trees infected with various citrus pathogens) potted trees was arranged on the lawn outside of the greenhouse under USDA, Animal and Plant Health Inspection Service (APHIS) regulatory approval and oversite over a 3-day period. Each replicated grid consisted of multiple non-infected citrus trees with randomly dispersed trees with *C*Las (positive control), *C*Laf (*Candidatus* Liberibacter africanus), various bacterial, viral, viroid, phytoplasma and spiroplasma diseases (Table 1). In addition, one tree from Brazil was assessed by the canines that was presumptively infected with *C*Lam (*Candidatus* Liberibacter americanus) but repeated qPCR of this tree for this pathogen have remained inconclusive. All four canines were presented with each non-target pathogen-infected tree at least twice in different grids to determine if specific training for *C*Las would result in false positive alerts on trees infected by non-target pathogens with symptoms and/or physiological manifestations similar to HLB decline. In this study canines were exposed to citrus pathogens infecting a range of scion cultivars, rootstocks, and citrus species.

A portion of the overall pathogen collection assessed by 4 canines is provided as an example. Over the 3-day study, 1944 trees were assessed by canines as shown in the latent class metric table. Relative to Table S2, the individual error calculations and latent class metrics for detection are shown in Figure S10.

J. Cross reaction studies of citrus infected with other *Liberibacter* sp. *C*Las infected trees in the collection originated from various countries including USA (Florida and California), Taiwan, Thailand, Vietnam, Reunion, Japan, Pakistan, and India, thus representing a diversity of *C*Las strains. For *Candidatus* Liberibacter solanacearum, 3 canines were interrogated 10 potted tomato plants in a row in which a single plant infected with *C.* Liberibacter solanacearum was randomly placed. The experiment was repeated once with a second *C.* Liberibacter solanacearum -infected tomato plant randomly placed. Neither canine reacted to either of the *C.* Liberibacter solanacearum –infected plants or any non-infected plants (0 FN) indicating that there was no cross reaction of canines trained on *C*Las with the *C.* Liberibacter solanacearum pathogen.

For *Liberibacter crescens*, budwood purportedly infected with the bacteria was obtained from the California Department of Food and Agriculture (CDFA) who had previously reported *L* crescens infected material from California (*44*) and transported under regulator permit to the USDA, Agricultural Research Service, Molecular Plant Pathology Laboratory in Beltsville, MD, where it was budded into non-infected sweet orange scions. Subsequently the presumptively *L. crescens*-infected trees were transported under regulatory permit to the USDA ARS Horticultural Research Lab in Fort Pierce, Florida for canine interrogation. Multiple post-graft transmission PCR assays conducted in Beltsville and in Fort Pierce were all negative for *L. crescens*, however, due to the prolonged subclinical nature of *Liberibacter sp.*, they were considered potentially *L. crescens*-infected. Eight and six HLB detector canines were used in two replicates of the experiment. In each replicate, 50 non-infected citrus were arrayed in 5 rows of 10 plants. One plant was randomly replaced with a known *C*Las-positive control and two were replaced with *L. crescens*-graft-inoculated trees. Each canine interrogated the grid four times during, with the infected/inoculated trees randomly rearranged each time. All canines correctly identified the *C*Las-infected trees (1.0000 accuracy) with no alerts on the presumptive *L. crescens*-inoculated plants with no FP or FN alerts.

K. Composition of the *C*Las-infected tree volatilome. Headspace sampling and gas chromatography-mass spectrometry (GC-MS) analysis was used to assess non-infected and *C*Las-infected tree volatilomes. Three mature leaves from non-infected and *C*Las-infected grapefruit seedlings (confirmed by qPCR) were removed and immediately used for volatile analysis. Each leaf was rolled and sealed in a 20-mL vial (7 cm in height) crimp capped with a silicone septum (Gerstel Inc., Linthicum, MD). After incubation for 30 min at 22° C, a 2-cm solid phase microextraction (SPME) fiber (50/30 μm DVB/Carboxen/PDMS; Supelco, Bellefonte, PA) was exposed to the headspace for 30 min. After exposure, the SPME fiber was inserted into the injector of a GC-MS (Model 6890; Agilent, Santa Clara, CA) to desorb the extract for 15 min at 250° C. The GC-MS equipment and settings were: DB-5 (60 m length, 0.25 mm i.d., 1.00 μm film thickness; J&W Scientific, Folsom, CA) columns, coupled with a MS detector (5973 N; Agilent).

The column oven was programmed to increase at 4° C·min−1 from the initial 40° C to 230° C, then ramped at 100° C·min−1 to 260° C and held for 11.7 min for a total run time of 60 min. Helium was used as carrier gas at a flow rate of 1.5 mL.min−1. Inlet, ionizing source and transfer line were kept at 250°, 230°, and 280° C, respectively. Mass units were monitored from 30 to 250 m/z and ionized at 70 eV. Data were collected using a data system (ChemStation G1701 AA; Hewlett-Packard, Palo Alto, CA). A mixture of C-5 to C-18 n-alkanes was run at the beginning of each day to calculate retention indices (RIs) (*59*). Volatile compounds were identified and quantified by comparison of their mass spectra with authentic volatile compound standards, and/or library entries (NIST/EPA/NIH Mass Spectral Library, version 2.0d; National Institute of Standards and Technology, Gaithersburg, MD), as well as by comparing RIs with published RIs (*61-66*) (Fig. S11, Table S3). As stated by Angle, "*Much more research needs to be conducted to understand the movement of biological VOC within the thermal plume (e.g., micro currents) and in the aerodynamic wake/wind currents in order to develop search patterns to optimize biomedical detection"* (*54*).

L. Canine detection of *C*Las in non-citrus host plants. For each non-citrus host (*Catharanthus roseus* (L.) G.Don – rosaceae and Madagascar periwinkle, *Nicotiana benthamiana* Domin – solanaceae, were interrogated by 4 canines. For *C. roseus* rows of 10 plants per row were interrogated by four canines with one *C*Las-positive *C. roseus* placed randomly in the row of non-infected *C. roseus* plants. The experiment was repeated 10X per canine using different *C*Las-infected plants in different random positions (Fig. S12A). . For *N. benthamiana* only a few plants were available. Therefore, a line of 10 stations was used composed of 8 potted citrus trees with a single *C*las-infected citrus in one position as a positive control and one *C*Las-infected *N. benthamiana* randomly placed in the line. Six canines interrogated 10 re-randomized lines (Fig. S10B).

M. Canine detection of *C*Las in bacterialiferous *Diaphorina citri* psyllid vectors. Psyllids from *C*Las-infected and non-infected populations were harvested from established colonies feeding on *C*Las-positive and non-infected potted citrus trees, respectively. Small tubular insect cages (10 cm long by 3 cm diameter) were used to contain 20 *C*Las+ or *C*Las-ACP each. One cage was placed in each of 10 open-top metal cans such that only a single randomly placed can contained 20 caged *C*Las-positive ACP. Three canines each interrogated the 10 cans, then the position of the *C*Las-positive cage was rerandomized and the canines reinterrogated all cans for a total of 9 replications per canine (Fig. S13).

N. Canine interrogation of axenic *C*Las bacterial culture. The presumptive coculture of *C*Las was established by coauther (Y.P. Duan) from *D. citri* gut microflora and contained multiple uncharacterized bacteria. The coculture was assayed via qPCR on the day of the canine assessement and found to have a Ct = 25.32 (estimated 6.79 X 10^5 copies/ml). The 200ul of the coculture as well as 10^{-4} (Ct=37.93) and 10^{-6} (Ct = non detectable) dilutions were pipeted onto sterile cotton filter paper discs and placed in individual metal cans. Controls were created by pipetting 200ul of sterile water on identical cotton discs. Pure cultures of *E. coli, Pseudomonas* sp., and an uncharacterized bacterial isolate were also prepared and 200ul pipetted onto cotton

filter discs at full strength as additional negative controls. Ten metal cans were arrayed in a line with random placement of one can with the *C*Las co-culture (at various dilutions), one or more cans with other pure bacterial cultures and the remainder with sterile water controls. Canines were allowed to run down each line interrogating all 10 cans in sequence. The entire experiment was repeated twice for 3 replications using 2 canines per replication over 2 days.

At full concentration all canines correctly allerted on the *C*Las co-culture with 1 FN and 0 FP alerts out of 120 targets assayed sensitivity = 0.9167, specificity = 1.0000 and acuracy = 0.9917 (Fig. S14A). Canines were also tested at 2 dilutions of the co-culture, 10^{-4} and 10^{-6}. At a dilution of 10^{-4}, *C*Las concentration was near the qPCR detection threshold and canines had 1 FN and 1 FP allerts out of 120 targets assayed, sensitivity = 0.8333, specificity = 0.9907 and acuracy = 0.9750 (Fig. S12B). At the lowest concentration tested, a dilution of 10^{-6}, concentrations of *C*Las were below qPCR detection threshold and yet canines still alerted on some of the targets; 5 FN and 2 FP alerts out of 120 targets assayed, sensitivity = 0.0.4167, specificity = 0.9907 and acuracy = 0.9333 (Fig. S14C). This lowest concentration contained less than a single copy of the *C*Las bacterium, indicating that the canines may be aleting on bacteria subcomponents (ex. proteins, peptides, metabolites, etc.) with more than one copy per bacterial cell. The probability (*P*) of correct indication of the co-culture by chance in repeated trials with multiple canines was $1x10^{-12}$, $1x10^{-12}$, and $1x10^{-24}$ for the full concentration, 10^{-4} and 10^{-6} dilutions, respectively.

O. Field validation and deployment for early detection in an emerging HLB epidemic. *Commercial citrus.* Canine *C*Las detection proficiency was assessed in commercial citrus orchards St. Lucie County, Florida. *C*Las and its vector ACP are endemic and widespread in Florida, and the majority of plantings exceeding 90% infection incidence. Therefore, to find plantings with low incidence, only newly established orchards less than 18 months old were used. A complete census of *C*Las infection was conducted in a ~4 ha block of 12-mo-old red grapefruit by collecting four leaves from each tree, assessing *C*Las infection via qPCR, and preparing a map of resulting estimated disease incidence. Each canine systematically assessed all trees in the study block to determine their sensitivity, specificity and other metrics as indicated above in a commercial citrus setting. As indicated above, canines are capable of detecting *C*Las infection weeks to months prior to our ability to confirm infection via qPCR. Canines frequently alerted on trees that were recorded as qPCR negative for *C*Las. Therefore the block was periodically reassessed via qPCR to allow us to determine if the canine alerts were true positives but subclinical to qPCR at the time of canine interrogation, or if the alerts were false positives. Thus in Florida the determination of canine detection accuracy was often offset by several months following the day on which the canines assessed the citrus orchard.

To more accurately examine canine detection of initial infections, i.e. early pathogen detection, 4, and 9 canines were transported to the commercial citrus growing area in the Rio Grande Valley of South Texas over two different trips, respectively, in 2016-2018. At that time in South Texas, *C*Las infection was widespread but early in the epidemic and thus remained in low incidence. The canines examined multiple commercial red grapefruit orchard blocks, and one experimental block

of red grapefruit located at the field site of Texas A&M University, Kingsville Citrus Center near Weslaco, Texas with 3785 trees assayed (Fig. S15).

Prior to and 1 mo. after canine assessment, the citrus blocks were assessed by qPCR to determine the spatial distribution of *C*Las-infected trees. Canines individually ran the qPCR-assessed rows interrogating all trees. Canines detected the previously confirmed *C*Las-infected trees (sensitivity = 0.7112, specificity = 0.9719 and accuracy = 0.9559), but multiple canines alerted on additional presumptive *C*Las-infected trees in the blocks as well. These presumptive *C*Las-infected trees were considered false positives for the purpose of calculating the latent class statistics. However, the majority of these were undoubtedly cryptic infections below the detection threshold of PCR to confirm *C*Las infection. Had we been able to retest these trees through time, it is highly probable that many would have been confirmed as *C*Las-positive, increasing the metrics for sensitivity, specificity, and accuracy of the assay considerably and more in line with prior tests where the disease status was known with certainty.

P. Residential citrus. The canines were trained for residential citrus survey in various urban locations in the Rio Grande Valley area of Texas. Although no PCR data were available to confirm canine detection accuracy in the majority of the residential areas where the canines trained, the location of a small number of confirmed *C*Las positive trees were known and utilized for training. Canines were also deployed to Los Angeles and Orange Counties of Southern California for residential detection validation studies in December 2018 and February 2019. Two or three canine and handler teams were deployed on each validation trip and canine teams worked closely with California Department of Food and Agriculture (CDFA) inspectors to gain official and sanctioned access to individual properties. Residential properties are very diverse environments with a broad range of plant species, age, size, and horticultural health, interspersed within a limitless variety of obstacles and other animals often encountered. Citrus trees in this environment may be planted directly in the soil or in pots and may be difficult to reach, requiring the canines to wind, squeeze and/or climb throughout a sometimes dangerous environment.

Over the two validation deployments, the canines examined 52 residential properties in *C*Las infected areas of Orange and Los Angeles Cos. CDFA had prescreened these properties and pre-assayed any presumptive citrus trees in the landscape via PCR. In addition, CDFA had obtained potted citrus trees of known *C*Las infection status (*C*Las-positive and *C*Las-negative) from the USDA, Agricultural Research Service Citrus Germplasm Repository in Riverside, California and placed them throughout the landscapes of the residential properties. These trees were unmarked and served as blinded true positive and true negative unknowns to the canine detection teams. For the two deployments, there were 19 and 14 blinded trees, respectively distributed within the residential properties. The blinded trees were destroyed immediately after the study to ensure no unintentional spread of *C*Las occurred within the residential environment. Canines performed well identifying the previously confirmed (PCR-positive) *C*Las-infected trees within the residential landscape and the blinded potted trees, sensitivity = 0.9024, specificity = 0.9394, accuracy = 0.9189 (Fig. S16). It was recognized that many *C*Las-infected trees likely resided within these residential properties that were below the qPCR detection threshold. These suspect canine

detections were not incorporated into the latent class analyses because the true *C*Las infection status was unconfirmed. There were many canine alerts on such trees, and their precise positions within the landscape of each property were recorded. In addition, CDFA immediately collected tissue from these trees and ran subsequent qPCR assays on them. Four additional *C*Las-infected trees on which the canines alerted were subsequently confirmed. CDFA will continue to re-assay the remaining suspect trees on which the canines alerted over time. It is highly probable that more of these trees will be confirmed through time as *C*Las-positive, rising the true sensitivity and accuracy of the assay to be more in line with prior canine performance in situations of known *C*Las incidence. This validation study demonstrates the keen canine early detection ability and underscores the utility of canine *C*Las detectors in diverse environments.

Q. Deployment strategies for detection of *C*Las in commercial orchards To ensure that canine detection is optimized, we normally run each canine along each row of trees, turning at the end of the row and entering the next, using a serpentine pattern to traverse all rows in sequence. This can be done with dogs on a leash controlled by the handler or off leash for more experienced canines familiar with the search pattern. The canines interrogate, (smell), each tree in sequence. When deployed in commercial citrus plantations, trees spacing within row are 2-4m depending upon species, density of planning, etc. As trees mature, they form long foliar hedgerows. Canine detectors are nearly instantaneous at scent recognition and alert on *C*Las-infected trees within 2-3 seconds. Although detection speed may be considered a less important metric of performance compared with accuracy, it should not be underestimated (*41*). Based on our experience using canines in commercial citrus orchards, canines interrogate at a rate of 2.26 +/-0.91 s per tree while trotting along rows. When they alert on a tree by sitting, the average reward time is 47.45 +/-16.37 sec, after which the canine is ready to resume the search. We use these values to extrapolate the time required to survey a standard 4.05 ha (10 acre) block of mature citrus consisting of 1470 trees (Table S4). Disease incidence affects reward time. The more diseased trees encountered, the more canine alerts occur, and the more reward time required. Thus as disease incidence increases from 0.5 to 5.0%, the time require to survey the entire block increases from 60.91 to 113.89 minutes, respectively. However, compared with the time to sample and process samples for molecular assay (ex PCR), serological assays, or even human visual assessment of individual trees, canines are very rapid.

R. Canine duty cycle. The durability of individual canines and the environmental conditions of the search area effect their duty cycle. Heat and humidity causes canines to pant which can divert some of the scent intake away from the nasal passages when odor is discriminated. Within the canine detection community, the most frequently stated duty cycle is 30 minutes followed by a rest period of similar duration (*62*). Interestingly, Gardner *et al.* demonstrated that within the context of their study, environmental and physiological variables were not strongly related to duty cycle measures. Two of four detector canines showed a statistically significant negative relationship between percent alerts and environmental temperature, and one canine showed a statistically significant positive relationship between percent alerts and body temperature. Gardner also found no statistically significant correlation between performance and relative humidity. In the Gardner study, all four canines were willing and able to work as long as asked and the

conditions of the study did not exceed the capabilities of the canines to work for extended periods. This demonstrated that within practical limits, dogs can work for extended periods of time if they are trained to do so. However, citrus is grown most often in warm to tropical climates. Therefore, we adopted a 30 min working, 30 min resting duty cycle to maintain optimal detection performance. Thus, every ~30 min., one team ends their survey cycle and another resumes the survey where the first team stopped. The first team rests for 30-60 minutes before resuming survey duties, etc. In practice, multiple teams are deployed in an area simultaneously to optimize survey time.

Occasionally there are adverse environmental variables with which canine teams must contend. Although canines are seemingly immune to rough brush, high grasses, or obstacles common in residential areas, handlers are often not so immune or require more time to avoid obstacles. Additionally, we found that some common orchard weeds (ex. *Tribulus terrestiris*, i.e. goatheads) have spines that can puncture the canine's footpads, requiring canines to wear fitted boots with durable rubber soles in some situations. The canines immediately adapted to and ignored the boots after a few minutes.

S. Simulations of deployment strategies. The spatial heterogeneity of HLB infections is related to ACP vector dispersal dynamics. Immigrating ACP populations preferentially accumulate at the periphery of citrus blocks and along orchard voids such as roads, canals, ponds, and staging areas devoid of trees, which coincide with initial *C*Las transmission and subsequent infections (*11,48,63-67*). Anco determined there was a slightly higher ACP population abundance along southern and eastern orchard edges comparted to northern and western edges that significantly corresponded to the phototactic response of psyllids to the seasonal azimuth/elevation of the sun (*48*). We can take advantage of this spatial heterogeneity for early detection of *C*Las infections when deploying canines.

We developed a series of deployment strategies that a canine detection company can provide to citrus producers and have calculated their relative detection efficacy. These are based on the known spatial distribution of HLB, which initially accumulates at the periphery of the block, i.e., edge effect, and simulations to calculate the probability of detection. Depending upon the need of the citrus grower (+/- presence of the pathogen versus determination of exact disease incidence), canines could be deployed in several different ways, ranging from a simple perimeter survey to a stratified complete census of all trees. Perimeter surveys are the quickest, and therefore the most economical. For example, for a single-tree depth perimeter survey versus a deep perimeter survey of the outermost 3 trees, the probability of detection is 0.7720 versus 0.9200. For a stratified survey of every 7th, every 3rd, versus every row the probability of detection increases from 0.7900, to 0.8740, to 1.0000, respectively (Fig. S17).

T. Assessment of canine deployment survey strategy. Prior spatial analyses demonstrated that *C*Las infections are spatially heterogeneous in commercial citrus orchards related to ACP vector dispersal dynamics (*64-67*). Immigrating ACP populations preferentially accumulate at the periphery of citrus blocks resulting in edge-associated patterns of *C*Las transmission and

subsequent infections. Therefore, for early detection of *C*Las infections in commercial orchards, we can exploit the use of peripheral surveys of entire plantations and individual internal blocks, preferentially, to take advantage of the significantly higher accumulation of infections on the periphery of orchard blocks. However, if the intent of the survey is to estimate the overall incidence of *C*Las infection, various stratified survey designs for canine olfactory detection can be employed. The more intensive the spatial stratification, the higher the probability of detection (Fig. S17). Finally, if the intent is to determine the incidence and precise location of *C*Las infection with the greatest accuracy possible for management decision making, a complete census survey is required (Fig. S17).

We investigated the validity and efficacy of different possible survey patterns for canine deployment using 2 years of temporal *C*Las infection data from a large south Florida citrus plantation. The data represent four surveys (each a complete visual census) for more than 250,000 citrus trees in 180 blocks (Fig. S18). The blocks are arranged in six rows of 30 blocks, and each block typically contains around ~1500 trees of the same age and variety. Symptomatic trees were identified through visual inspection by experienced surveyors, and their inspection accuracy was in good agreement with PCR confirmation. It is worthy to note that visual inspection may not detect exposed, latent or cryptic *C*Las-infected trees.

To optimize sampling effort, canines are deployed initially to survey a sub-sample of trees within the citrus block, either via perimeter or stratified survey. If any *C*Las-infected trees are detected in the pre-screen survey, a subsequent complete census survey is conducted for the *C*Las-positive block. Therefore, we will only select *C*Las-positive blocks with 0-5% DI for analysis of survey performance. Data of the spatial distribution of *C*Las was used from a previous study (*38*). Totally, we have 451 citrus blocks selected from the plantation across the four survey time points (Fig. S18 A,B,C). Citrus orchards are planted in rows and as trees mature branches interlock and form large hedgerows. Thus, the canine and human handler teams are constrained along the rows and cannot easily cross between rows except at the block periphery. We take this into account by developing either perimeter or stratified S shape serpentine survey patterns (Fig. S17, S18 C,D). We varied the sampling density for both canine survey strategies to compare their *C*Las detection performance (e.g. perimeter surveys of 1, 2, 3…7 tree depth and compared with stratified surveys via serpentine patterns of each 2^{nd} row, 3^{rd} row…7^{th} row). For each selected citrus block, we calculated the number of *C*Las-infected trees encounters under the proposed survey pattern.

Binomial distribution theory and simulation were used to determine the detection accuracy of the perimeter and various stratified designs deployment strategies in Figures S15 and S16. Note when we use a perimeter survey of 7 trees deep and stratified survey of every row both surveys provide a complete census surveys. For each 4 ha block, each of the four corners was used as a possible starting position for canine deployment. The efficacy of detection via these survey strategies was estimated considering a range of canine detection accuracy, 1-(FN+FP), of 0.05 to 1.0, where 1.0 = 100% accuracy with no errors and 0.05 = 5% accuracy (Table S5). Results demonstrated that if we consider vector-biased spatial distribution of *C*Las infection in commercial orchards and assume 95% canine detection accuracy, perimeter survey was superior to stratified survey for

confirmation of *C*Las-infected tree presence and ranged from 76.6 to 99.5 percent reliability of detection when disease incidence is <2% for perimeters 1-7 trees deep (Table S5). For the lowest intensity canine surveys, 1 tree deep perimeter versus every 7th-row stratified survey, in 2.4 ha (10 ac) orchard block canines would pass by and interrogate ~232 versus ~312 trees or 16 versus 21% of the planting, for perimeter versus stratified survey, respectively. This equates to 24% less trees interrogated with a commensurate savings in deployment time.

U. Simulation of spatiotemporal dynamics of *C*Las-infection to compare the efficacy of *C*Las control using visual inspection, PCR, and canine detection. Mathematical modeling and geospatial technologies are able to grasp the spatiotemporal complexity of pest and disease invasion dynamics as well as the implementation and evaluation of management programs. Based on previous modeling frameworks and analyses (*68*-*71*), we use a spatially explicit, stochastic, individual-based compartmental (SECIR) model to simulate *C*Las spread across a commercial citrus landscape. Citrus hosts are classified by disease status: Susceptible, Exposed, Cryptic (infectious, but asymptomatic), Infected (infectious and symptomatic), and Removed, whereas, the ACP vector is modeled as a relative density ρ(t) at the orchard-level to incorporate general population dynamics (e.g., endemic or seasonal/cyclic populations) affecting transmission risk. Thus, the instantaneous rate of exposure for a susceptible host *i* at time *t* is given by

$$\varphi_i(t) = \rho(t)\left[\varepsilon + \beta \sum_j K(d_{ij}, \alpha)\right]$$

where the summation runs over all infectious hosts *j*. The parameters ε and β represent the primary (external) and secondary rates of infection. The function $K(d_{ij},\alpha)$ defines an isotropic dispersal kernel where d_{ij} is the distance from susceptible host *i* to infectious host *j*, and α is a scaling parameter. For the *C*Las infection simulation study, an exponential dispersal kernel was used. We use a host orchard landscape of 5,616 trees in a 6-block formation representing a commercial citrus grove with an initial, low incidence of *C*Las-infected trees (selected randomly or introduced along the borders, i.e. edge effect of vector transmission), and an endemic ACP population for the simulation analysis. Simulation design and parameterization determined by input from citrus growers/production managers, diagnostic laboratories, and survey managers are shown in Fig. S19.

Survey and removal are the sole controls implemented in this simulation study to investigate the efficiency of *C*Las detection techniques. Survey deployment options include survey design (e.g., full census, perimeter/edge, stratified), timing/frequency, and detection technique. The temporal probability/efficiency of *C*Las detection for canines and PCR was determined via data analyzed from the canine early detection study discussed above. Canines detected *C*Las-infection in 70% of the host plants in the first month and all plants at six months after infectious ACP exposure. PCR detected maximally 54% host plants infected with *C*Las at 5 and 10 months post-exposure; however, PCR confirmed on average just 20% at any given time point (Fig. 3). This pattern of *C*Las detection via PCR is indicative of the sampling issue (i.e., selecting the right tissue for assay) when the disease is not yet systemic in the host plant.

Curves were fitted to the data with variable ranges to present best- and worst-case scenarios on detection probability for each technique (Fig. S20A). Additionally, we consider visual survey as a third detection technique. Bassanezi modeled the relationship between tree age and symptom development that we use to constrain visual detection probability as well as augment PCR sampling efficiency (and thereby increasing detection probability over time as the infection progresses within a host) (*72*) (Fig. S20B):

$$s(t) = \frac{1}{(1 + \left(\frac{1}{s_0} - 1\right) e^{-rt})}$$

After disease confirmation, removal of infected trees is the primary combatant in reducing the local inoculum pressure. Removal strategy options include removal of individually confirmed *C*Las-positive trees and culling around detections. It is important to note that both infection confirmation (i.e., lab capacity for sample processing) and removal often occur after variable time delays; to account for this variability, lab confirmation and removal times can be sampled from normal distributions with a specified mean and standard deviation, and restricted by a maximum delay for mandatory removal (e.g. within 30 days). Additional scenarios were investigated to analyze the impact of delayed removal protocols on orchard sustainability when paired with canine deployment (Figs. S21, S22, S23). Tree replacement of removed hosts can be incorporated to investigate replanting scenarios for replacing lost citrus production. Replanting options include timing and frequency as well as criteria to stop a replanting program (e.g. maximum resets allowed per landscape or per host). For the simulation studies when replanting was implemented, we assumed tree replacement occurred annually during the first quarter of the year for any hosts removed in the previous year due to *C*las infection (Fig. S24).

Costs were integrated into the model to analyze the sustainability of each simulated detection program. Survey, removal and replanting cost ranges were determined via consultations with commercial survey companies and citrus industry experts. Detector canine costs can vary by the number of canine-handler teams deployed and survey design. PCR costs include sample collection, lab processing, technician salaries, infrastructure costs, etc. Visual assessment or scouting can vary by acreage, frequency and multi-pest survey design. Removal and replanting costs were defined on a per tree basis. Additionally, noting the host variety/cultivar, planting density and age, the production outputs and costs were estimated from compiled data from growers and regulatory agencies. Yield is also impacted by *C*Las infection. To estimate the relative yield, Bassanezi established a general relationship between symptom severity and relative yield of an HLB-infected tree in Brazil (*50*).

$$y = e^{-1.85x}$$

To conduct comparative economic analyses of detection technologies, we implement a full survey of the host landscape every 180 days. Additionally, we reduce the canine detection probability

toward a worst-case scenario and shift PCR detection probability toward a best-case scenario (Fig. 4). A side-by-side comparison of each detection program scenario conducting a full survey twice per year with the same initial conditions (10 Exposed hosts located on the edges) and individual infected tree removal within 30 days of detection were simulated (Fig. 4, Movie 7). We also examined different initial conditions (edge versus random distribution of initial *C*Las-infected trees) and removal protocols for each detection program (Figs. S21, S22). As the delay in mandatory removal post detection increased, canine deployment is less impactful on orchard sustainability (although dramatically better than PCR or visual) as the detected inoculum sources are allowed to continue propagation before being removed. Mandatory removal within 90 and 120 days of detection resulted in ~48% and ~36% healthy trees remaining in the orchard, respectively, when canines were deployed. On the other hand, swift removal within 30 days post detection resulted in more than 90% healthy hosts (Figs S21, S22).

Simulations were subsequently run 10,000 times to estimate the proportion of disease-free (Susceptible) hosts, total trees removed annually, and the 95% confidence intervals for the operating profit per acre over the course of the epidemic given 10 initial edge introductions and removal within 30 days of detection via each technique (Fig. S23, Movie S8) and given 10 random infections with canine deployment and different removal deadlines (Fig. S22). We also explored a similar simulation of the three *C*Las detection methods (canine, PCR and visual), with and without annual replacement of infected trees that accumulated over each prior year (Figs. S23,S24, respectively).

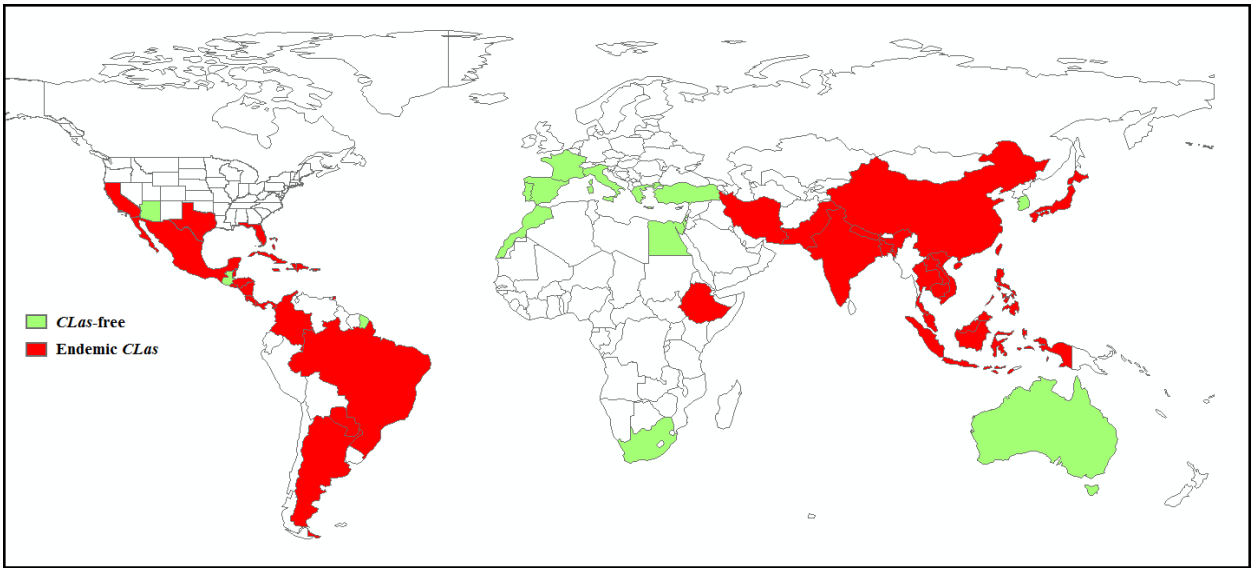

Fig. S1. Citrus producing counties and presumptive distribution of *C*Las - causal agent of citrus Huanglongbing (HLB).

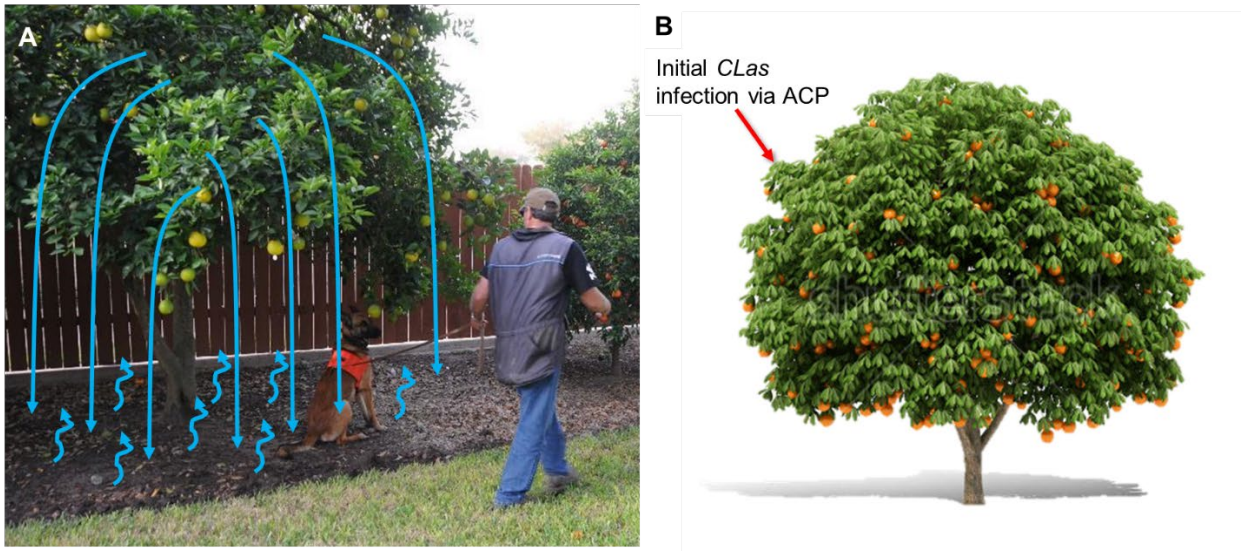

Fig. S2. Holistic interrogation of *C*Las-infected trees by canine detectors. A. Early detection via canines is devoid of sampling issues. The volatile scent signature associated with *C*Las-infection settles from the canopy and simultaneously emanates from root infections pooling at the base of the tree. The canine detector interrogates the tree holistically by alerting on the scent signature regardless of its origin, i.e., a single leaf, root, stem or the entire tree if systemically infected. B. Conversely, other detection technologies, eg. PCR, are reliant on selecting and assaying a small amount of tissue from large trees and often miss incipient infections.

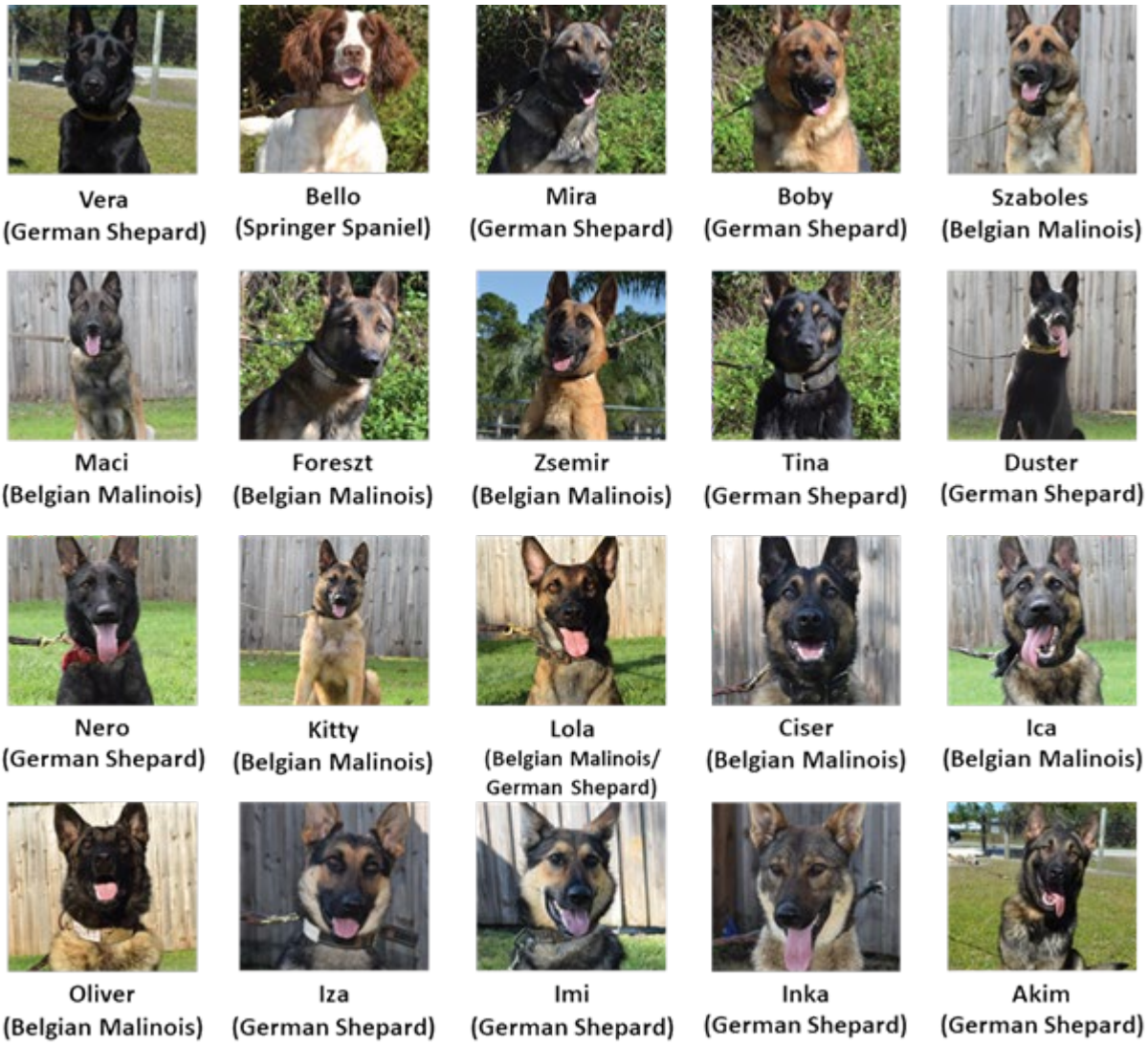

Fig. S3. Group of 20 canines trained to detect *C*Las-infected citrus trees. Various combinations of these canines were used throughout the experiments described in the paper.

660

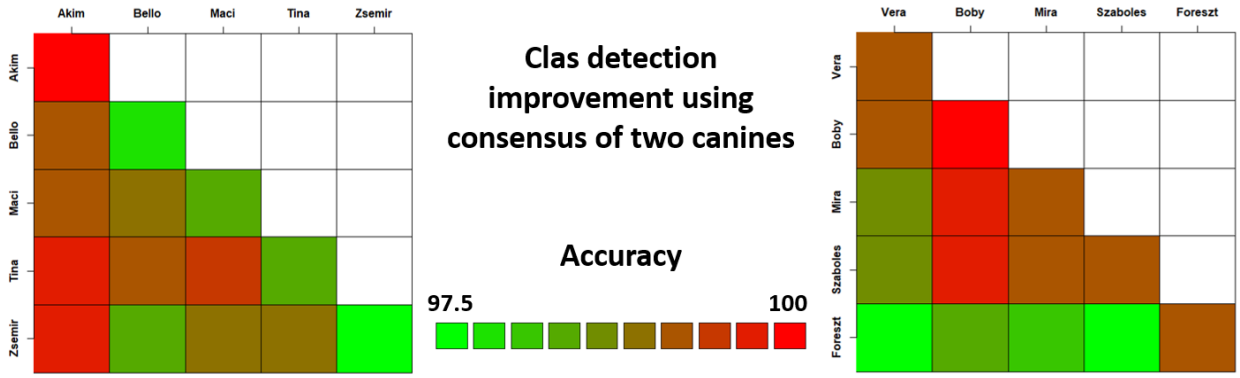

Fig. S4. Results of consensus sampling by multiple canines. Overall accuracy of canine *C*Las detection improves when using consensus of two or more canines. Data from 10 canines used in various combinations.

665

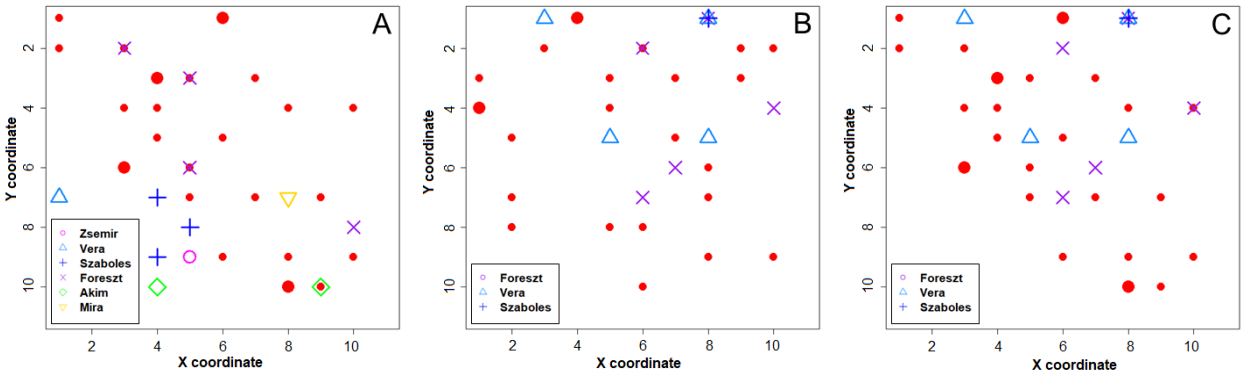

Fig. S5. Spatial proximity of false canine detector FP errors to prior positions of TP *C*Las-infected tree positions by canine. Small red and large red dots, prior position of single and multiple *C*Las-infected trees, respectively. Other markers indicate FP detection alert of individual canid (by given name) per legend. Marker overlaying red dot indicates FP canine alerts at prior position of *C*Las-infected tree in prior trial. See Fig 2, error calculated over 10 canines for *C*Las detection over 10 trials of 100 trees each, i.e. each canine interrogated 1000 trees.

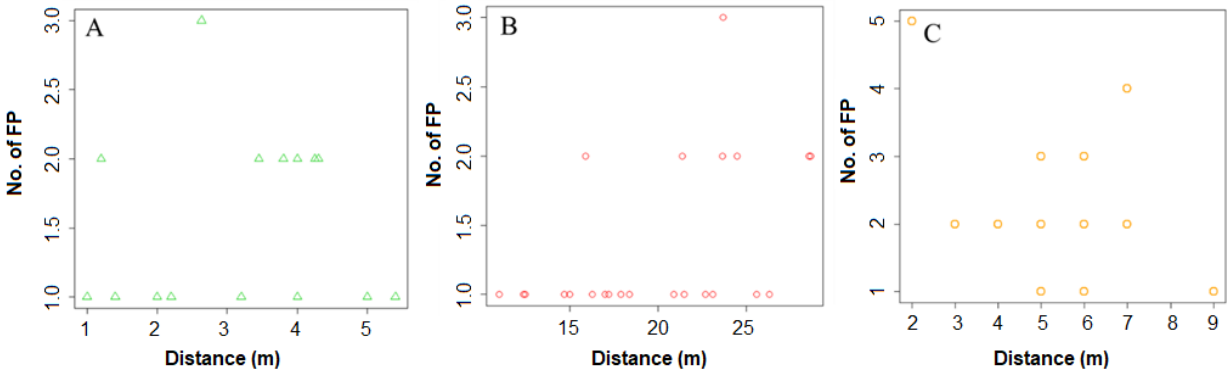

675 **Fig. S6. Spatial proximity of false positive (FP) indicated by *C*Las detector canines.** A. Distance to the closest *C*Las-infected tree. B. Distance to all *C*Las-infected trees. C. Distance of FN alerts to perimeter of study plot. See Fig 2, error calculated over 10 canines for CLas detection over 10 trials of 100 trees each, i.e. each canine interrogated 1000 trees.

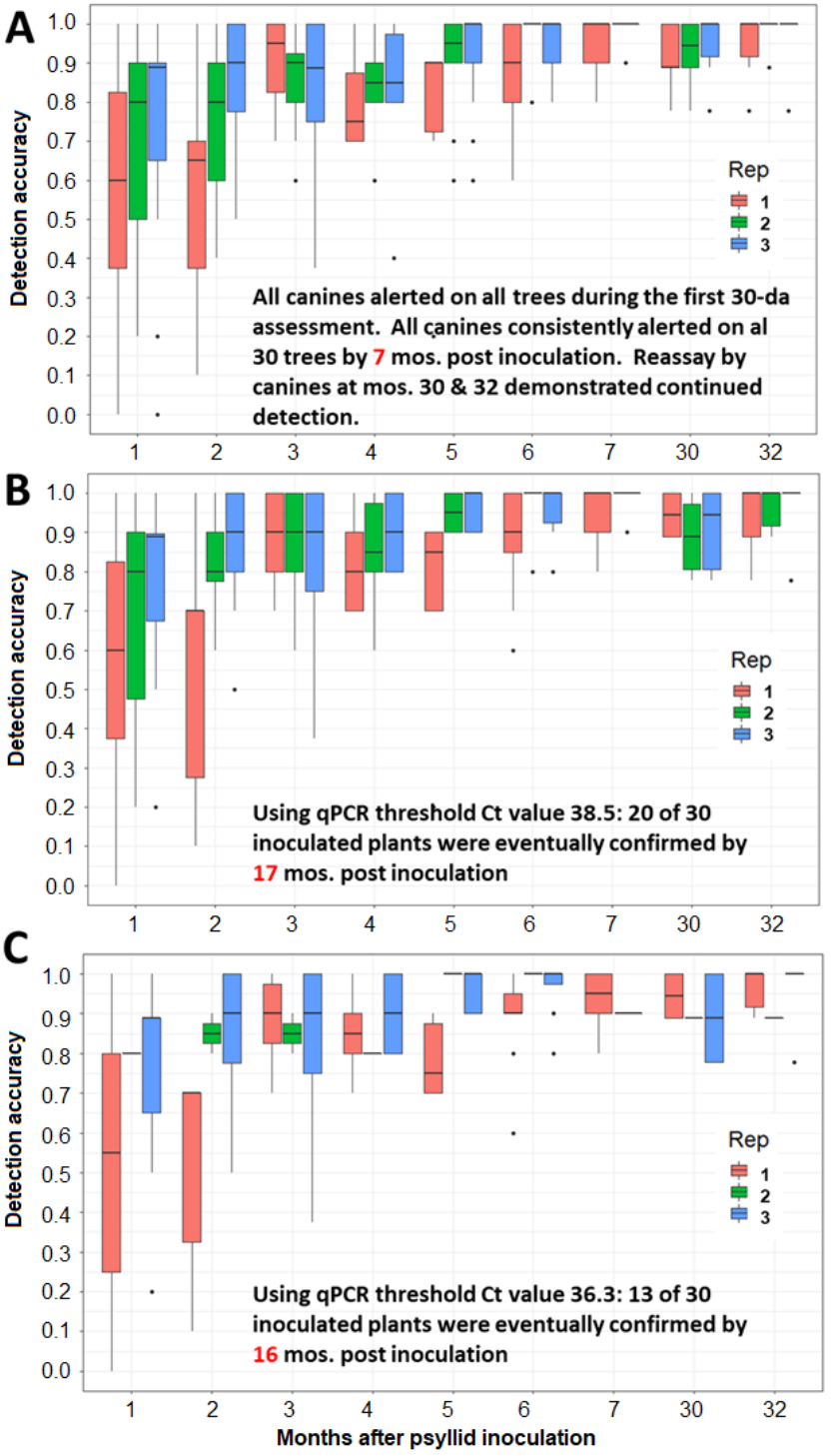

680

Fig. 7. Canine detection accuracy by monthly assay date. Canine assays were replicated 3 times on each assay date using 10 canines. A. Canine detection results irrespective of qPCR confirmation. B. Canine detection results considering qPCR confirmation using regulatory threshold of Ct < 38.5, and C. Ct < 36.3 Once canine detection reached an optimum at 7 months
685 canine assays were discontinued but resumed at 30 and 32 months to demonstrate that canines as a group maintained at >90% detection over time.

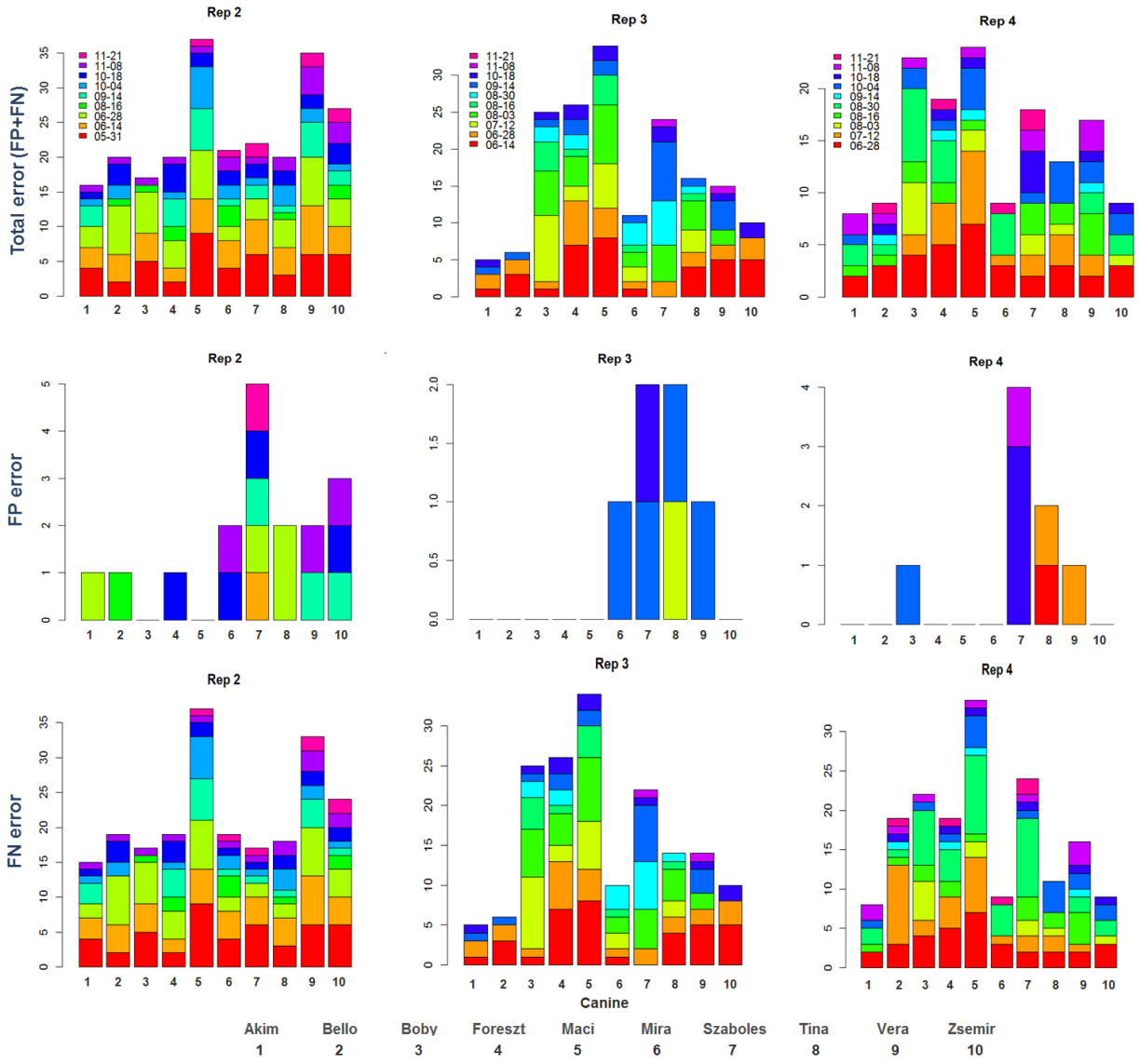

Fig. S8. Temporal assessment of canine subclinical detection of *C*Las-infection. Assessment of error associated with subclinical detection of *C*Las-infection. Total error, FP and FN error associated with each of 10 canines for three replicates of the experiment (Top panel row). Each bar is cumulative error across all assay dates. Color within each bar denotes error contributed by individual assay date.

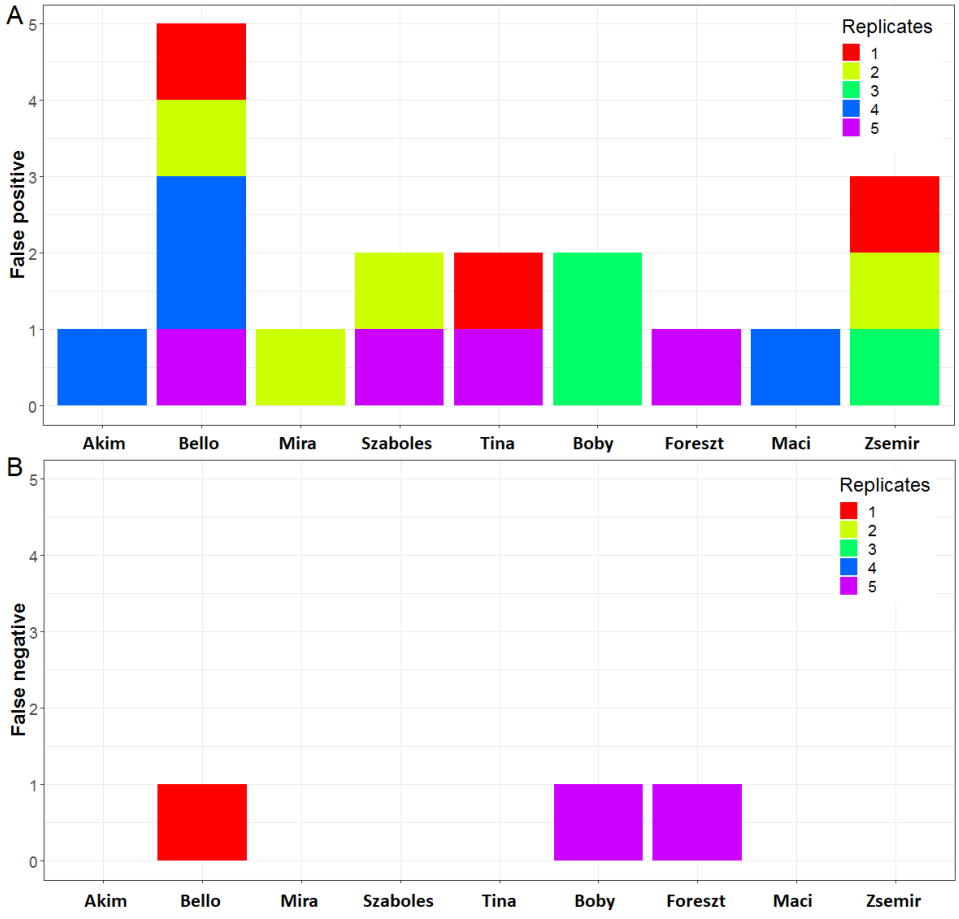

C	Canine diagnostic test outcomes				TP	72
		True Condition			TN	1032
		+	-		FP	3
Canine Assay		90	1035		FN	18
+	75	72	3		SEN	0.8000
-	1050	18	1032		SPC	0.9971
					PPV	0.9600
1125	Total population (*n*)				NPV	0.9829
1.9%	Total Error Rate				FPR	0.0029
1.6%	False Negative Error Rate				FDR	0.0400
0.3%	False Positive Error Rate				ACC	0.9813

Fig. S9. Canine detection of *C*Las-infection from root tissue. Each of 9 canines interrogated 5 replications of 25 root samples with 2 *C*Las-infected samples in each 25-sample grid. Color within each bar indicates contribution of individual replicate to: A. false positive, or B. false negative error. C. Latent class metrics for canine detection of CLas-infected in Root tissue compiled over 5 replicates.

B	Canine diagnostic test outcomes				TP	139
		True Condition			TN	1795
		+	-		FP	5
Canine Assay		144	1800		FN	5
+	144	139	5		SEN	0.9653
-	1800	5	1795		SPC	0.9972
					PPV	0.9653
1944	Total population (*n*)				NPV	0.9972
0.5%	Total Error Rate				FPR	0.0028
0.3%	False Negative Error Rate				FDR	0.0347
0.3%	False Positive Error Rate				ACC	0.9949

Fig. S10. Canine discrimination of *C*Las from other infectious citrus pathogens. A. Four canines interrogated *in vivo* *C*Las and other infectious citrus pathogens from the exotic citrus pathogen collection housed at USDA, ARS in Beltsville, Maryland over 3 days. B. Latent class metrics for canine detection of *C*Las-infected accessions complied over a 3-day trial.

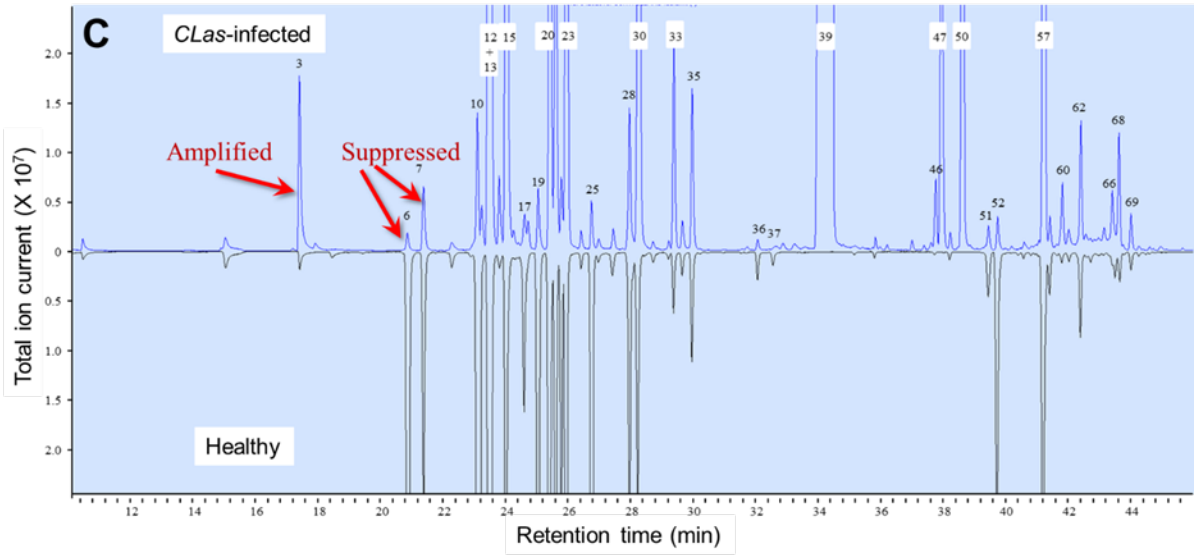

Fig. S11. Volatile organic compound (VOC) assay of *C*Las-infected versus healthy trees. C. Comparison of VOCs from *C*Las-infected (blue) and healthy (black) Marsh grapefruit leaves via GC-MS. Note some VOCs are up-regulated 'amplified' and others down regulated 'suppressed' in *C*Las-infected leaves (Table S3 and S Methods).

A	Canine diagnostic test outcomes			TP	72
		True Condition		TN	720
		+	-	FP	0
Canine Assay		80	720	FN	8
+	72	72	0	SEN	0.9000
-	728	8	720	SPC	1.0000
				PPV	1.0000
800	Total population (*n*)			NPV	0.9890
1.0%	Total Error Rate			FPR	0.0000
1.0%	False Negative Error Rate			FDR	0.0000
0.0%	False Positive Error Rate			ACC	0.9900

B	Canine diagnostic test outcomes			TP	6
		True Condition		TN	54
		+	-	FP	0
Canine Assay		6	54	FN	0
+	6	6	0	SEN	1.0000
-	54	0	54	SPC	1.0000
				PPV	1.0000
60	Total population (*n*)			NPV	1.0000
0.0%	Total Error Rate			FPR	0.0000
0.0%	False Negative Error Rate			FDR	0.0000
0.0%	False Positive Error Rate			ACC	1.0000

Fig. S12. Latent class metrics for canine detection of *C*Las-infected non-citrus hosts. A. *Catharanthus roseus* data compiled over 2 replications, each using 4 canines and 10 runs of 10 plants/run to interrogate the mixed *in vivo*-infected/non-infected plant populations. B. *Nicociana suaveolens (benthamiana)* data for 6 canines that interrogated a line of 10 plants composed of 8 *C*Las-negative citrus, one *C*Las positive citrus (positive control) and one *C*Las-infected *N. benthamiana* randomly placed in the line.

	Canine diagnostic test outcomes				TP	46
		True Condition			TN	482
		+	-		FP	8
Canine Assay		50	490		FN	4
+	54	46	8		SEN	0.9200
-	486	4	482		SPC	0.9837
					PPV	0.8519
540	Total population (*n*)				NPV	0.9918
2.2%	Total Error Rate				FPR	0.0163
0.7%	False Negative Error Rate				FDR	0.1481
1.5%	False Positive Error Rate				ACC	0.9778

Fig. S13. Latent class metrics for canine detection of *C*Las-bacterialiferous Asian citrus psyllids. Data compiled over 2 days, each using 3 canines, 9 repetitions of 10 cans/repetition. Each can (station) held a cage containing a population of 20 *C*Las-positive or *C*Las-negative psyllids.

A	Canine diagnostic test outcomes			TP	11
		True Condition		TN	108
		+	-	FP	0
Canine Assay		12	108	FN	1
+	11	11	0	SEN	0.9167
-	109	1	108	SPC	1.0000
				PPV	1.0000
120	Total population (*n*)			NPV	0.9908
0.8%	Total Error Rate			FPR	0.0000
0.8%	False Negative Error Rate			FDR	0.0000
0.0%	False Positive Error Rate			ACC	0.9917
				P	1.00E-12

Full concentration	
qPCR Ct =	25.32
Copy No. =	135722

B	Canine diagnostic test outcomes			TP	10
		True Condition		TN	107
		+	-	FP	1
Canine Assay		12	108	FN	2
+	11	10	1	SEN	0.8333
-	109	2	107	SPC	0.9907
				PPV	0.9091
120	Total population (*n*)			NPV	0.9817
2.5%	Total Error Rate			FPR	0.0093
1.7%	False Negative Error Rate			FDR	0.0909
0.8%	False Positive Error Rate			ACC	0.9750
				P	1.00E-12

Full concentration	
qPCR Ct =	37.93
Copy No. =	51

C	Canine diagnostic test outcomes			TP	5
		True Condition		TN	107
		+	-	FP	1
Canine Assay		12	108	FN	7
+	6	5	1	SEN	0.4167
-	114	7	107	SPC	0.9907
				PPV	0.8333
120	Total population (*n*)			NPV	0.9386
6.7%	Total Error Rate			FPR	0.0093
5.8%	False Negative Error Rate			FDR	0.1667
0.8%	False Positive Error Rate			ACC	0.9333
				P	1.00E-24

Full concentration	
qPCR Ct =	ND
Copy No. =	0

Fig. S14. Latent class metrics for canine detection of *C*Las co-culture. A. Co-culture at full strength and B. Co-culture diluted to 10^{-4}, and C. Co-culture diluted to 10^{-6}, below qPCR detection thresholds. Data compiled over 2 days, 3 replications per day of 10 stations per replication, using 2 canines per replication. Copy number was calculated for 200µl of co-culture solution, the volume pipetted onto filter pads and interrogated by each canines. *P* = probability of correct indication of the co-culture by chance in repeated trials with multiple canines.

	Canine diagnostic test outcomes				TP	165
		True Condition			TN	3453
		+	-		FP	100
Canine Assay		232	3553		FN	67
+	265	165	100		SEN	0.7112
-	3520	67	3453		SPC	0.9719
					PPV	0.6226
3785	Total population (*n*)				NPV	0.9810
4.4%	Total Error Rate				FPR	0.0281
1.8%	False Negative Error Rate				FDR	0.3774
2.6%	False Positive Error Rate				ACC	0.9559

Fig. S15. Latent class metrics for canine detection of *C*Las in canine commercial citrus orchard blocks in Weslaco, Rio Grande valley of South Texas, USA. Data were compiled over 2 separate multi-day trips to Texas using 4, and 9 canines per trip, respectively, and using multiple commercial citrus blocks. Data presented are a compilation of total trees interrogated by one or more canines over all trips.

A	Canine diagnostic test outcomes			TP	25
		True Condition		TN	18
		+	-	FP	1
Canine Assay		28	19	FN	3
+	26	25	1	SEN	0.8929
-	21	3	18	SPC	0.9474
				PPV	0.9615
47	Total population (*n*)			NPV	0.8571
8.5%	Total Error Rate			FPR	0.0526
6.4%	False Negative Error Rate			FDR	0.0385
2.1%	False Positive Error Rate			ACC	0.9149

B	Canine diagnostic test outcomes			TP	12
		True Condition		TN	13
		+	-	FP	1
Canine Assay		13	14	FN	1
+	13	12	1	SEN	0.9231
-	14	1	13	SPC	0.9286
				PPV	0.9231
27	Total population (*n*)			NPV	0.9286
7.4%	Total Error Rate			FPR	0.0714
3.7%	False Negative Error Rate			FDR	0.0769
3.7%	False Positive Error Rate			ACC	0.9259

C	Canine diagnostic test outcomes			TP	37
		True Condition		TN	31
		+	-	FP	2
Canine Assay		41	33	FN	4
+	39	37	2	SEN	0.9024
-	35	4	31	SPC	0.9394
				PPV	0.9487
74	Total population (*n*)			NPV	0.8857
8.1%	Total Error Rate			FPR	0.0606
5.4%	False Negative Error Rate			FDR	0.0513
2.7%	False Positive Error Rate			ACC	0.9189

Fig. S16. Latent class metrics for canine detection of CLas in residential citrus properties in Orange and Los Angeles Cos. of Southern California, USA. Latent class metrics shown for A. validation trip 1, B. validation trip 2, and C. overall. Each residence was interrogated by 2 canines, and a third canine was used to resolve any conflict in detection. All data from the 2-3 canines per residence utilized in metric calculations.

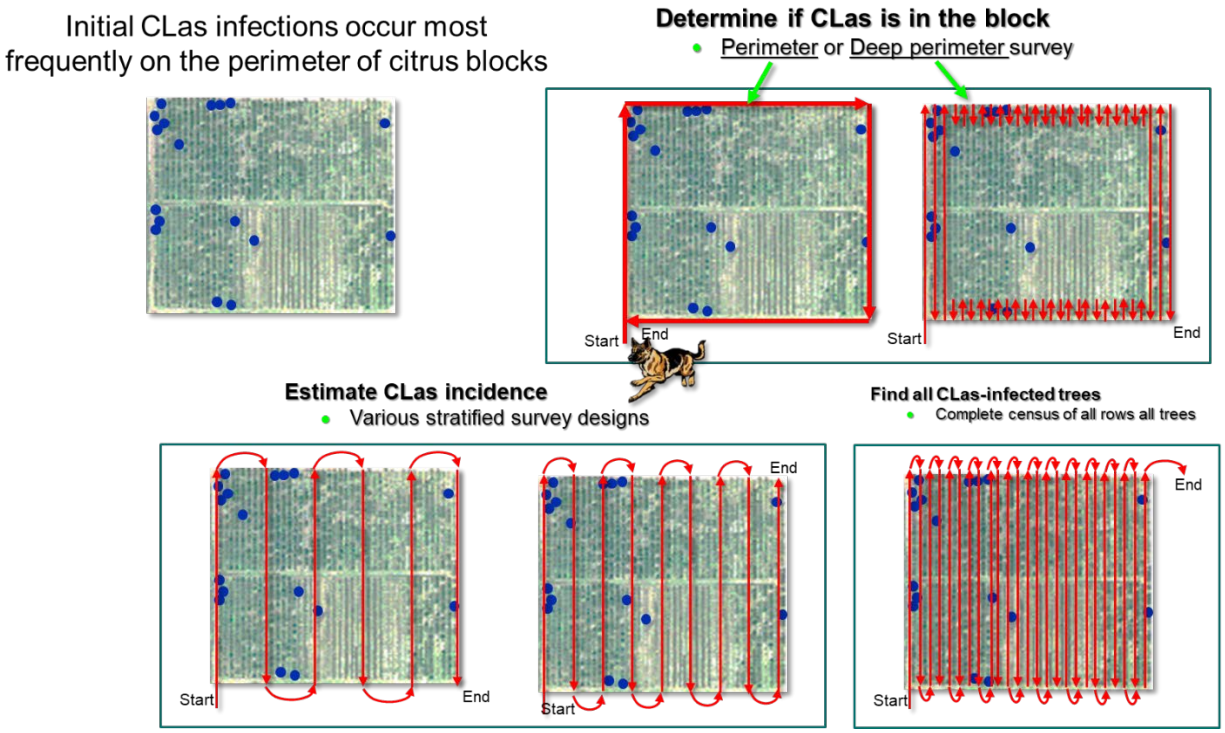

Fig. S17. Canine deployment strategies for *C*Las detection. Example citrus orchard with initial heterogeneous spatial distribution of *C*Las-infected trees indicated as blue dots (Top left). Perimeter (outer row and trees at end of row) and deep-perimeter (outer 2-3 rows and 2-3 trees at each end of rows) survey designs, path of canine detection team indicated by red arrows (Top center and right). Stratified survey designs at various intensity for estimation of *C*Las incidence (Bottom right and center). Complete census survey for greatest accuracy estimate of *C*Las infection and location of all known *C*Las-infected trees (right). Simulation results - percent detection of HLB (*C*Las infection) using various deployment strategies of 138 citrus blocks with <2% *C*Las infection.

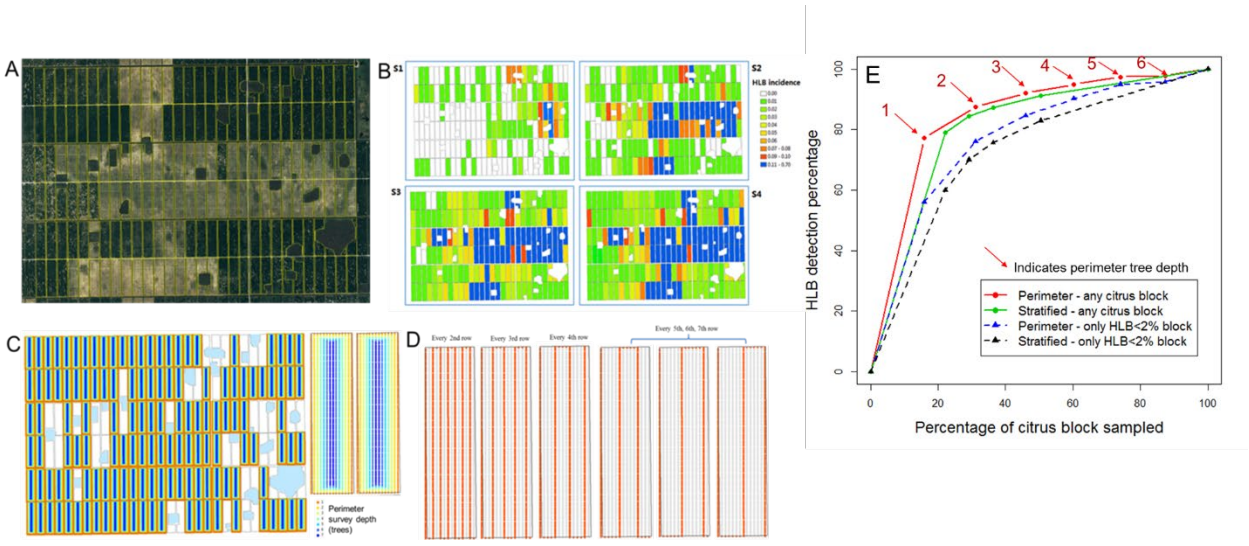

Fig. S18. Simulation of deployment strategies of *C*Las detector canines. A. Large citrus orchard in South Florida used for basis of simulation study consisting of 180 10-acre blocks. B. Graphical representation of the orchard showing diseases incidence of each block during four visual temporal assessments from November 2006 to March 2007. The spatial position of 451 *C*Las-infected blocks was used to assess survey method performance. C. Perimeter survey design of various depth in different colors. D. Stratified survey designs of varying intensity used for comparison. E Percentage of *C*Las-infected trees detected versus percentage of total citrus block surveyed.

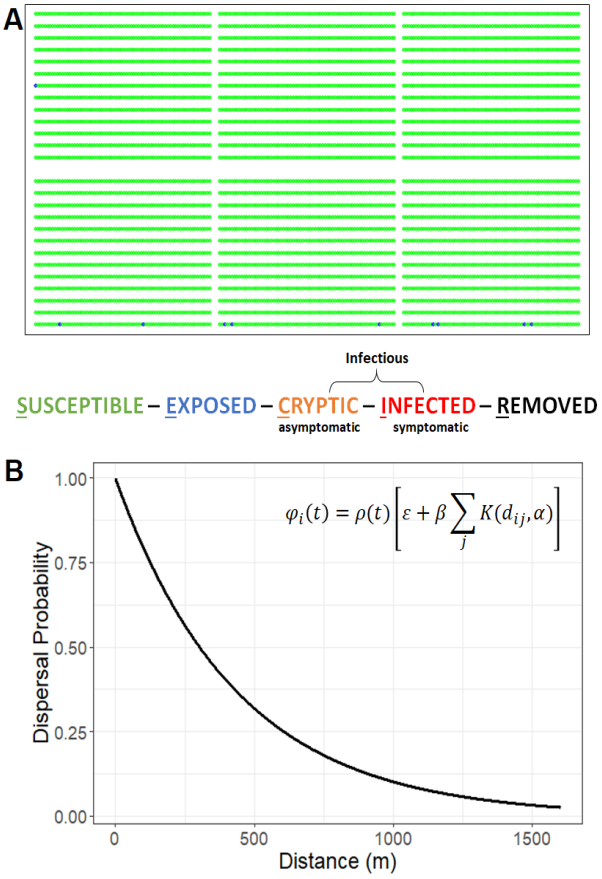

C

Parameter		Value	
Host Landscape		Approx. 40 acres	
Simulation Time		10 years	
Initial Conditions	<1% incidence	10 Exposed Hosts	
Survey Scheme		Full	
Survey Frequency		2 surveys/year	
Survey Cost	Canines	$7.50/tree	$5-10
	qPCR	$37.50/sample	$20-40
	Visual	$15/acre	$5-15
Removal Strategy		Individual	
Removal Delay	Canines	Immediate	
	qPCR	Simulated distribution (mandatory within 30 days)	
	Visual	Immediate	
Removal Cost		$150/tree	
Replant Time		1 replanting/year	
Site preparation and Replant Cost		$100/tree	
Bin return		$300	
Bins		40 bins/acre	
Production Cost		$3600/acre	

780 **Fig. S19. SECIR model simulation design and parameterization. A.** Host landscape with randomly simulated 10 initial *C*Las-exposed trees on the lower border of the planting indicated by blue dots, healthy trees green dots. B. Generalized psyllid dispersal of *C*Las over distance. C. Parameter values used to populate the model based actual management costs (can be redefined by user). Simulations run 10,000 times to generate outputs for Figs. 4, S22, S23, S24.

785

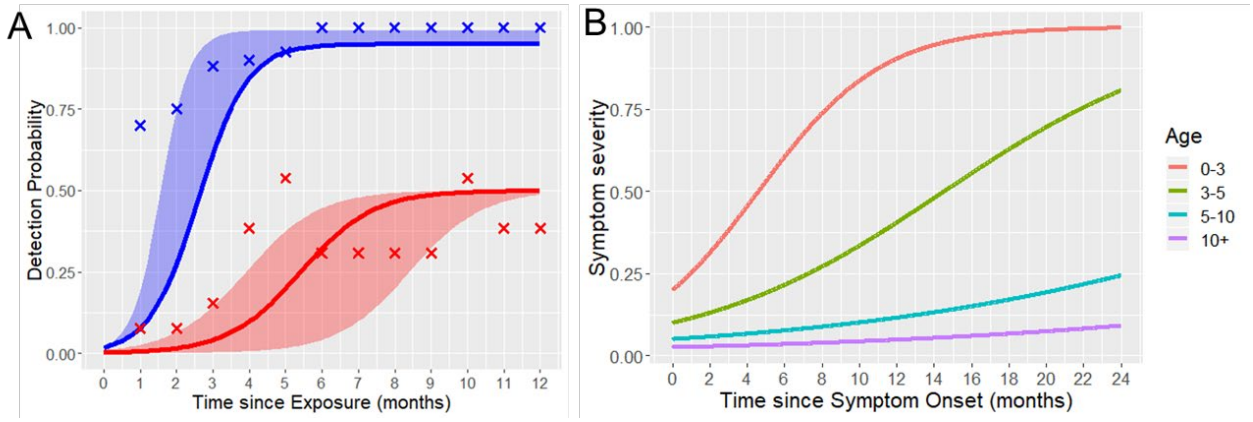

Fig. S20. Probability of detection of *C*Las infection of citrus trees over time based on visual, PCR and canine detection methods. A) Simulation settings for canines (blue line) and PCR (red line) detection within the range determined via psyllid study data. B) Symptom development with citrus host canopy based on tree age augmenting detection.

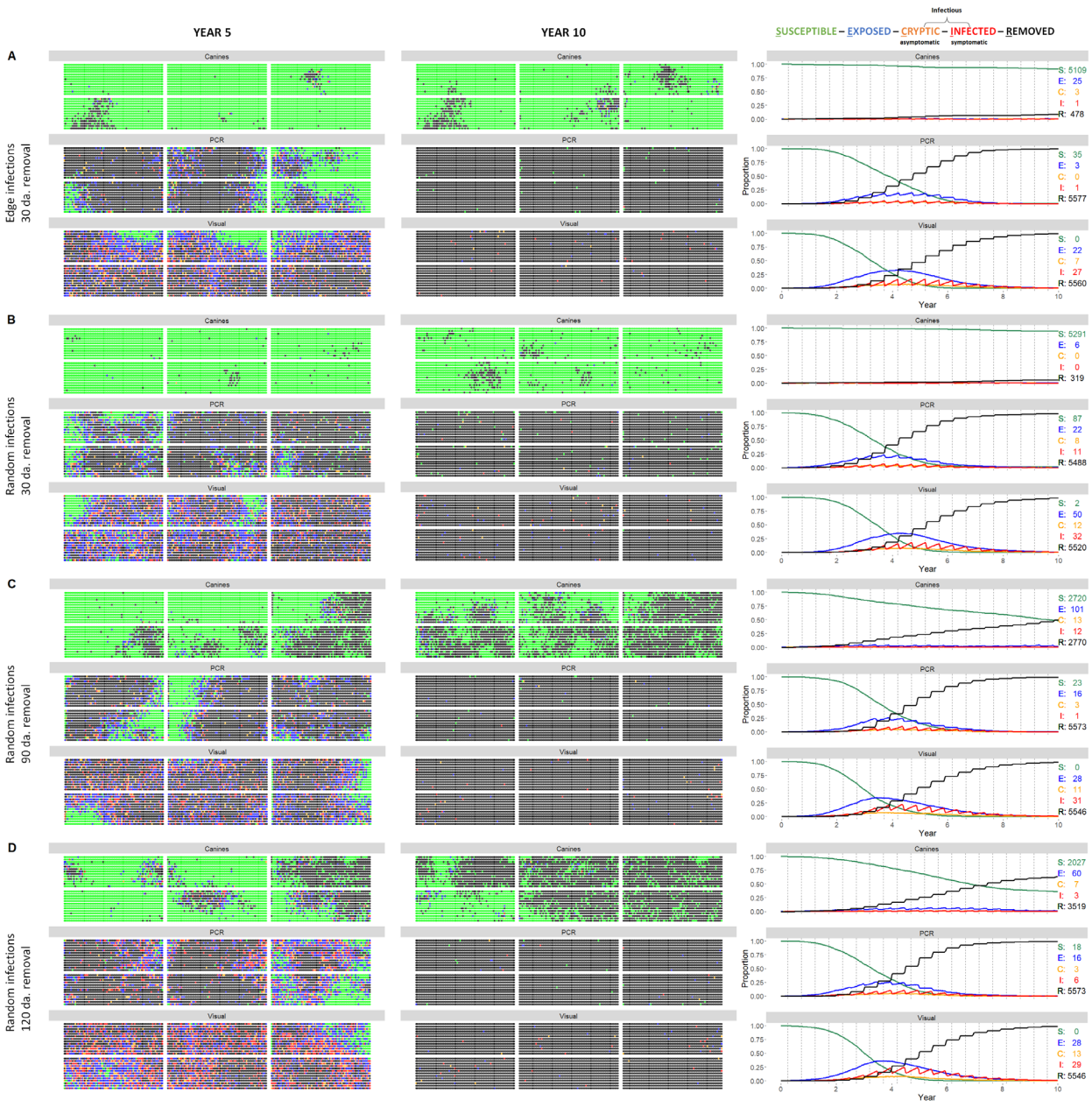

Fig. S21. Simulation scenarios investigating initial conditions and removal protocols over a 10 year period. Results from a single simulation run of (A) 10 initial edge infections and removal within 30 da. post detection, (B) 10 random infections and removal within 30 da. post detection, (C) 10 random infections and removal within 90 da. post detection, and (D) 10 random infections and removal within 120 da. post detection. Epidemic snapshots of the orchard at 5 and 10 year time points, and the disease dynamics with resulting tree numbers by disease status for each scenario.

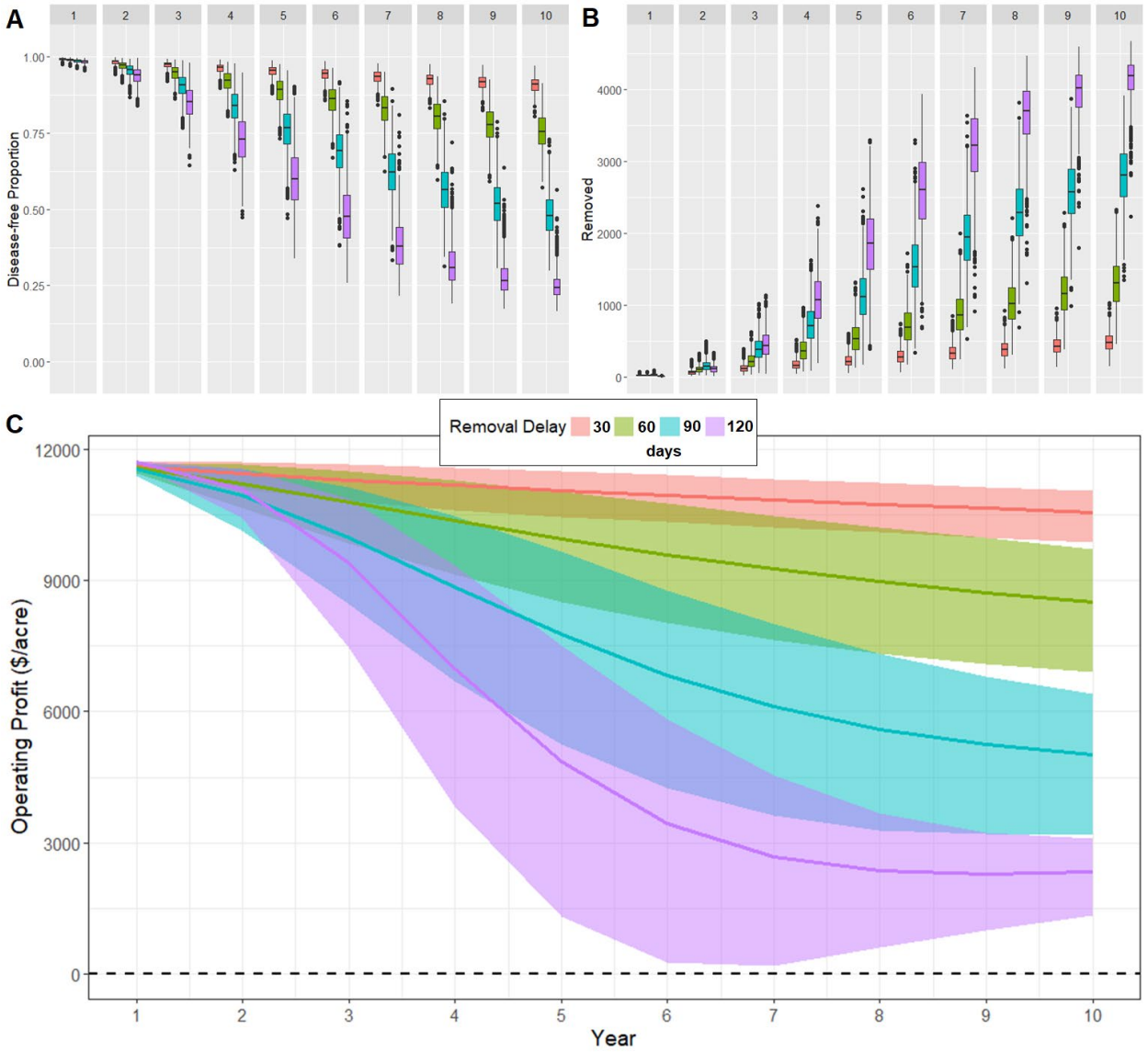

Figure S22. Simulation study over a 10-year period comparing removal programs coupled with canine deployment. Simulations were run 10,000 times to determine the (A) proportion of Susceptible hosts remaining, (B) number of trees removed post detection, and (C) 95% confidence intervals of the operating profit per acre each year when deploying canines with removal protocols mandating detected trees removal within 30 (red), 60 (green), 90 (blue), and 120 (purple) days. Simulations consider 2 surveillance cycles/yr, and operating profit calculations starting at the end of the first year. Dashed horizontal line denotes threshold of commercial citrus production operating profit/loss. Comparisons indicate that early detection paired with relatively prompt removal is required for long-term sustainability.

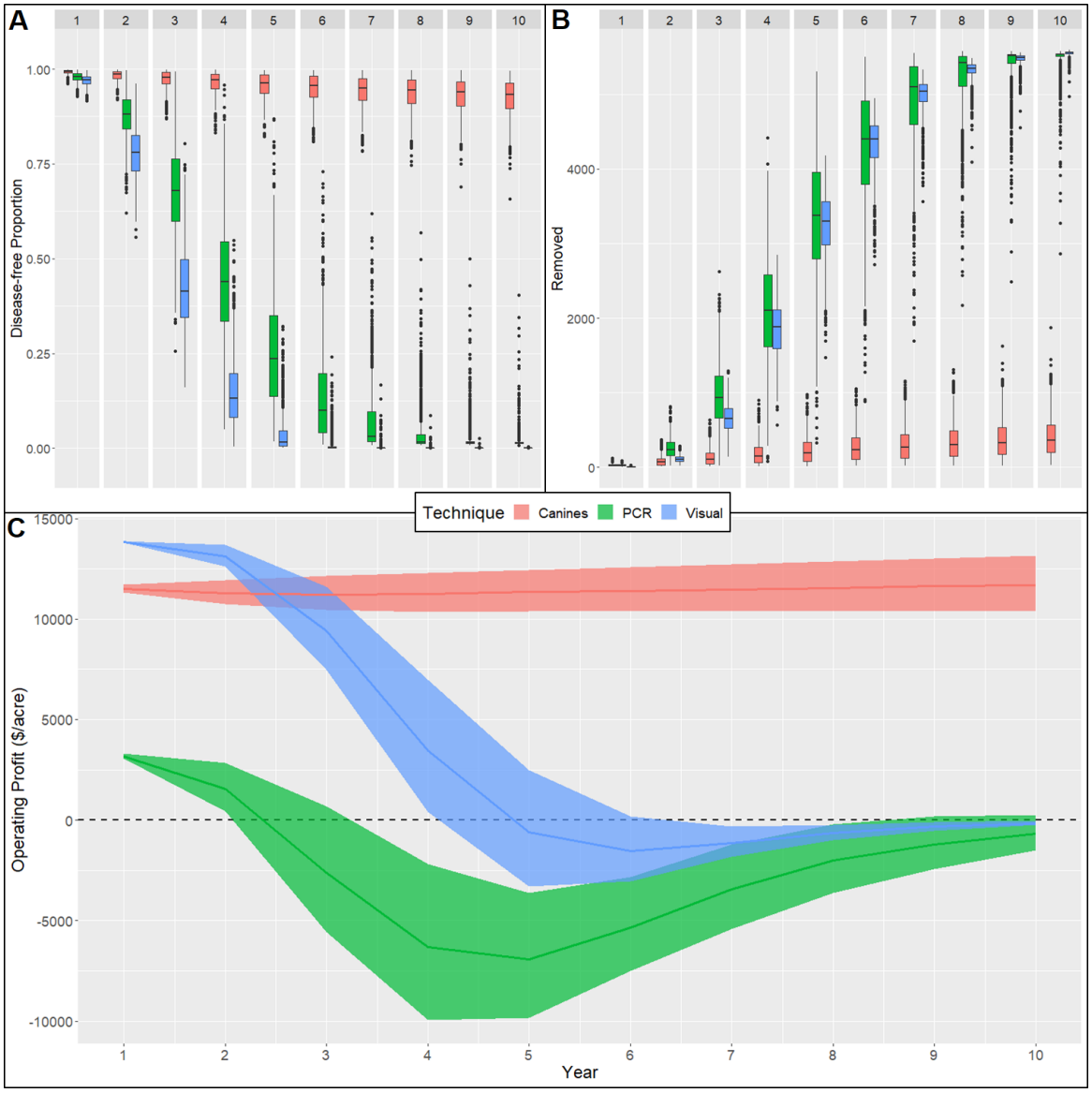

Fig. S23. Simulation study over a 10-year period comparing early detection technologies and their program sustainability without infected tree replacement. Simulations were run 10,000 times to determine the (A) proportion of Susceptible hosts remaining, (B) number of trees removed post detection, and (C) 95% confidence intervals of the operating profit per acre each year for canines (red), PCR (green), and visual (blue) scenarios. Simulations consider 2 surveillance cycles/yr, removal of infected trees within 30 days of discovery, without replacement of infected trees, and operating profit calculations starting at the end of the first year. Dashed horizontal line denotes threshold of commercial citrus production operating profit/loss. Note that profits are initially highest and lowest for visual and PCR detection because they are the least and most expensive, respectively. For visual and PCR scenarios, operating cost exceed earnings resulting in negative profits during year 3-10 for PCR and 5-10 for visual, returning to near zero profits at the end of 10 years. As 10 years is approached, there are only few trees left to surveil with PCR and visual detection, thus there are few fiscal outlays but no income when using either detection method, whereas, canine detection sustains both viable plantings and long-term profits.

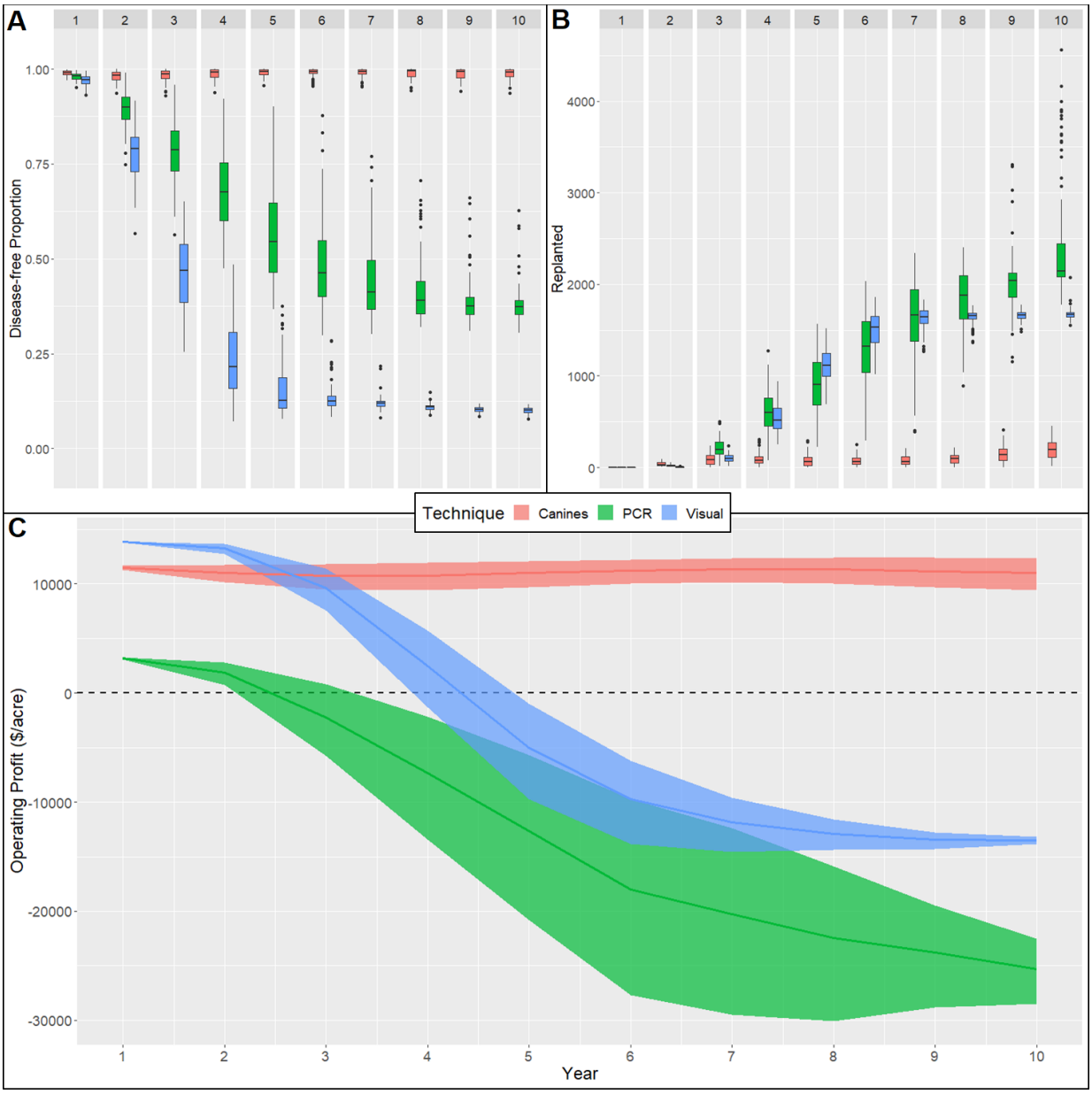

Fig. S24. Simulation study over a 10-year period comparing early detection technologies and their program sustainability with infected tree replacement. Simulations were run 10,000 times to determine the (A) proportion of Susceptible hosts remaining, (B) number of trees replanted, and (C) 95% confidence intervals of the operating profit per acre each year for canines (red), PCR (green), and visual (blue) scenarios. Simulations consider 2 surveillance cycles/yr, removal of infected trees within 30 days of discovery, replacement of cumulative prior-year infected trees once per year, and operating profit calculations starting at the end of the first year. Dashed horizontal line denotes threshold of commercial citrus production operating profit/loss. Note that profits are initially highest and lowest for visual and PCR detection because they are the least and most expensive, respectively. For visual and PCR scenarios, operating cost exceed earnings resulting in negative profits during year 3-10 for PCR and 5-10 for visual, returning to near zero profits at the end of 10 years.

Table S1. Performance assessment metrics for *C*Las-infected tree detector canines[a].

	Canine Detector										
Performance Metric	Akim	Bello	Masi	Tina	Zsemir	Vera	Bobby	Mira[b]	Szaboles	Foreszt	All canines
True Positive (TP)	38	32	33	32	28	36	36	16	35	40	326
True Negative (TN)	956	956	957	958	957	954	960	479	956	951	9084
False Positive (FP)	4	4	3	2	3	6	0	1	4	9	36
False Negative (FN)	2	8	7	8	12	4	4	4	5	0	54
Sensitivity- True Positive Rate (SEN)	0.9500	0.8000	0.8250	0.8000	0.7000	0.9000	0.9000	0.8000	0.8750	1.0000	0.8579
Specificity - True Negative Rate (SPC)	0.9958	0.9958	0.9969	0.9979	0.9969	0.9938	1.0000	0.9979	0.9958	0.9906	0.9961
Precision - Positive Predicted Value (PPV)	0.9048	0.8889	0.9167	0.9412	0.9032	0.8571	1.0000	0.9412	0.8974	0.8163	0.9006
Negative Predictive Value (NPV)	0.9979	0.9917	0.9927	0.9917	0.9876	0.9958	0.9959	0.9917	0.9948	1.0000	0.9941
False Positive Rate (FPR)	0.0042	0.0042	0.0031	0.0021	0.0031	0.0063	0.0000	0.0021	0.0042	0.0094	0.0039
False Negative Rate (FNR)	0.0500	0.2000	0.1750	0.2000	0.3000	0.1000	0.1000	0.2000	0.1250	0.0000	0.1421
False Discovery Rate (FDR)	0.0952	0.1111	0.0833	0.0588	0.0968	0.1429	0.0000	0.0588	0.1026	0.1837	0.0994
Accuracy (ACC)	0.9940	0.9880	0.9900	0.9900	0.9850	0.9900	0.9960	0.9900	0.9910	0.9910	0.9905

No single performance metric can capture all aspects of canine detection. Throughout this study we key on three commonly cited metrics; *sensitivity*, *specificity* and *accuracy* (outlined in red) with best and worst results among the 10 canines for each of these metrics indicated by green and red shading, respectively. However, we calculate and present a number of performance metrics in order to allow the reader to examine and interpret canine detection accuracy from various perspectives.

[a] Latent class metrics results from combined 10 trials per canine consisting of a 100 tree matrix with 0.04 incidence of *C*Las-infected trees randomized within the matrix. The 10 replicates per canine were pooled to estimate mean and variance for that canine.

[b] With the exception of one canine, who only participated in 5 of the 10 trials due to illness.

Table S2. HLB detector canine cross-reaction studies at USDA, ARS International citrus pathogen collection Beltsville, MD.

A

Accession	Pathogen/sample description	Origin	Virus/Viroid
B1	*CLas*	Reunion	
B49	*CLas*	South Africa	
B104	CRSV-6B-1	Florida	Ringspot
B121	*CLas Likubin*	Taiwan	
B141	*CLas*	Phillipines	
B144	*CLas*	China	
B232	*CLas*	Thailand	
B239	*Clas* From SU, HYd-cy-1	Taiwan	
B244	TLV code SATdw-JC-3	Taiwan	TLV, CTV
B245	TLV code WN-86-2	Taiwan	TLV
B246	ACD 17.GF/Tri - T. Roberts	Australia	ACD, CTV?
B251	Citrus Variagated Chlorosis	Brazil	CVC, CTV
B259	Dwarfing Agent	Argentina	Viroid/CTV?
B260	Dwarfing Agent	Argentina	Viroid/CTV?
B267	*CLas*	China	
B332	CCDV (Citrus Chloritic Dwarf)	Turkey	CCDV
B384	FS596 Meyer Lemon	Florida	TLV, CTV
B427	*CLas*	Brazil	
B428	*CLas* Rough Lemon Sample	Florida	
B429	*CLas* Valencia Sample	Florida	
B430	*CLas*	Japan	
B431	Stellenbosch	South Africa	
B432	ITSC Dark Valencia	South Africa	
B434	Nelspruit	South Africa	
B435	Letaba	South Africa	
B436	*CLas* Sour Orange Sample	Florida	
B437	*CLas* Dover #4 - Ron Brlansky	Florida	
B438	Hacienda Heights first CA find	California	
B439	*CLas* via CA from Tyler Dang	China	
B440	*Clas* - Sagheer Atta	Pakistan	
B441	*CLas San Gabriel 41 42 Mandarin 150416*	California	
B442	*CLas* from India via California	India	
B443	California 23 24 Mex lime 150416B	California	
B444	California 32 34 Calamondin 150416C	California	
B445	Claf HMV-5 via Fort Deterick - V. Damsteegt	South Africa	
189 Sw1	Stubborn Georgios Vidilacus	California	*S. citri*
3291-7	*CLas*	California	
Liberty	Stubborn - R. Yokomi	California	*S. citri*
S616	Stubborn Georgios Vidilacus	California	*S. citri*

B

Origin	Pathogen CTV	Pathogen *CLas*	Origin	Pathogen CTV	Pathogen *CLas*
USA			**Australia**	1	
California	17	5	**South America**		
Florida	6	4	Argentina	1	
Hawaii	8		Brazil	11	
Mediterranean			Colombia	10	
Corsica	1		Peru	14	
France	1		Venezuela	3	
Spain	22		Belize	1	
Turkey	1		**Caribbean**		
Asia			Bermuda	2	
China	15	2	Costa Rica	6	
India	14	1	Cuba	8	
Japan	10		Dominican Rep.	18	
Philippines	3	1	Guatemala	1	
Indonesia	2		Jamaica	1	
Malaysia	1		Puerto Rico	6	
Pakistan		1	Trinidad	1	
Taiwan	17	2	**Africa**		
Thailand	1	1	South Africa	11	4
			Reunion	1	1
			Totals	**246**	**22**

C

Canine diagnostic test outcomes		True Condition +	True Condition -
Canine Assay		144	1800
+	144	139	5
-	1800	5	1795

1934	Total population (*n*)	
0.5%	Total Error Rate	
0.3%	False Negative Error Rate	
0.3%	False Positive Error Rate	

TP	139
TN	1795
FP	5
FN	5
SEN	0.9653
SPC	0.9972
PPV	0.9653
NPV	0.9972
FPR	0.0028
FDR	0.0347
ACC	0.9949

A. Partial list of pathogens assessed by canines. B. number of isolates tested by country of origin. C. Latent class metrics for canine detection of *C*Las and cross-reaction to other citrus pathogens.

Table S3. GC-MS analysis of *C*Las-infected versus healthy grapefruit *Citrus paradisi* leaf volatiles.

Peak #	Compound	RT (min)	RI	Abundance		Peak #	Compound	RT (min)	RI	Abundance	
				HLB	Healthy					HLB	Healthy
1	Penten-3-one	10.48	695	6.12	3.93	38	(E,E)-2,4-Nonadienal	32.86	1226	4.39	0.00
2	(Z)-3-Hexenal	14.87	802	10.22	16.19	39	Linalool acetate	34.11	1259	4830.38	0.00
3	(Z)-3-Hexen-1-ol	17.56	865	97.33	10.52	40	Geranial	34.62	1272	13.61	0.00
4	1-Henaxol	17.90	872	4.23	0.00	41	Tridecane	35.75	1302	4.63	2.66
5	Bleed	18.46	885	1.10	4.59	42	Bornyl acetate	35.99	1309	1.15	0.00
6	α-Thujene	20.84	940	9.82	543.19	43	Linalyl propanoate	36.99	1337	4.57	0.00
7	α-Pinene	21.35	952	36.58	126.54	44	δ-Elemene	37.38	1348	2.15	0.00
8	Camphene	22.26	973	7.68	10.47	45	Linalool isobutanoate	37.61	1354	4.06	0.00
9	Benzaldehyde	22.87	986	4.45	2.65	46	p-Mentha-2,4(8)-diene	37.76	1358	34.47	1.42
10	Sabinene	23.09	991	68.50	1096.47	47	Neryl acetate	37.96	1364	386.62	0.00
11	Bleed	23.23	995	24.12	18.11	48	α-Cubebene	38.22	1371	8.10	3.53
12	Myrcene	23.43	999	512.44	244.72	49	24.19 7-epi-Sesquithujene	38.47	1379	0.84	0.00
13	ß-Pinene	23.53	1002	1012.55	204.70	50	Geranyl acetate	38.65	1384	586.76	0.00
14	Methyl-5-hepten-2-ol	23.78	1007	38.76	10.00	51	α-Copaene	39.44	1407	12.57	27.01
15	(Z)-3-Hexenyl acetate	24.05	1014	590.35	277.22	52	ß-Elemene	39.73	1416	16.62	174.03
16	Hexyl acetate	24.25	1018	11.88	0.00	53	ß-Panasinsene	40.19	1429	2.00	0.00
17	α-Phellandrene	24.60	1026	22.09	75.66	54	Sativene	40.38	1435	0.88	1.34
18	δ-3-Carene	24.71	1029	15.04	0.00	55	(Z)-Caryophyllene	40.58	1441	5.36	3.00
19	α-Terpinene	25.03	1036	32.37	387.67	56	γ-Elemene	41.06	1456	3.98	1.42
20	p-Cymene	25.43	1046	453.71	337.35	57	(E)-Caryophyllene	41.24	1462	709.51	249.56
21	Limonene	25.60	1050	250.12	260.26	58	ß-Muurolene	41.41	1467	17.36	20.72
22	ß-Phellandrene	25.78	1054	35.09	147.67	59	ß-Gurjunene	41.63	1474	3.35	1.62
23	(Z)-β-Ocimene	25.98	1059	791.18	378.52	60	Aromadendrene	41.79	1479	38.12	5.43
24	(E)-β-Ocimene	26.41	1068	8.77	7.05	61	(E)-ß-Ionone	42.01	1485	16.61	4.94
25	γ-Terpinene	26.74	1076	21.12	508.15	62	α-Humulene	42.39	1498	65.93	40.19
26	Isolimonene	26.98	1082	5.49	6.04	63	α-Farnesene	42.63	1505	12.12	2.15
27	p-Mentha-3,8-diene	27.43	1093	11.22	14.01	64	Germacrene D	43.13	1522	19.82	0.70
28	Terpinolene	27.96	1105	77.01	149.81	65	γ-Muurolene	43.28	1526	0.00	0.96
29	Perillene	28.04	1107	0.00	8.61	66	α-Muurolene	43.40	1530	41.76	5.42
30	Linalool	28.28	1113	570.12	133.46	67	ß-Selinene	43.47	1533	0.00	12.91
31	Nonanal	28.42	1116	0.00	0.00	68	α-Selinene	43.60	1537	57.51	14.09
32	1,3,8-p-Menthatriene	29.21	1135	4.36	3.70	69	δ-Cadinene	43.99	1550	17.25	9.26
33	(E,E)-allo-Ocimene	29.38	1139	101.10	28.07	70	(Z)-Calamenene	44.26	1559	1.66	1.90
34	(Z)-Limonene oxide	29.65	1146	15.73	11.70	71	(E)-Cadina-1,4-diene	44.58	1570	1.70	0.84
35	Camphor	29.97	1154	75.26	48.51	72	(E)-Nerolidol	44.89	1580	2.35	0.00
36	Terpinen-4-ol	32.06	1206	5.32	12.33	73	γ-Eudesmol	45.64	1606	1.03	0.00
37	α-Terpineol	32.57	1219	5.99	7.18		Total			11866.42	5680.13

RT and RI represent retention time and retention index, respectively. Note some VOCs concentrations in infected tissue are amplified, some are suppressed, while others are unaffected (red text indicates amplified/suppressed examples).

Table S4. Estimated canine detection of *C*Las infections considering sampling speed, reward time, duty cycle and the effect of disease Incidence (DI).

Total trees per 4.05 ha (10 ac) block	Interrogation time/tree (s)	Reward time/ detection (s)	*C*Las Incidence (DI)	Total *C*Las-positive trees rounded up	Total Reward Time (s)	Total Reward Time (min)	Total Survey incl. reward time (min)
1470	2.26 ± 0.91	47.45 ± 16.37	0.005	7	332.2	5.54	60.91
			0.01	15	711.8	11.86	67.23
			0.02	29	1376.1	22.93	78.30
			0.05	74	3511.3	58.52	113.89

Table S5. Results of simulation of canine detection accuracy for perimeter and stratified survey designs.

Canine Accuracy	Perimeter						
	1	2	3	4	5	6	7
1	0.772	0.876	0.920	0.949	0.973	0.978	1.000
0.95	0.767	0.870	0.915	0.944	0.968	0.973	0.995
0.9	0.761	0.864	0.910	0.938	0.963	0.969	0.990
0.85	0.756	0.858	0.904	0.932	0.957	0.963	0.984
0.8	0.749	0.851	0.898	0.926	0.950	0.958	0.978
0.75	0.742	0.843	0.891	0.919	0.943	0.951	0.972
0.7	0.734	0.836	0.884	0.912	0.935	0.945	0.964
0.65	0.725	0.827	0.876	0.904	0.927	0.937	0.956
0.6	0.715	0.818	0.867	0.895	0.918	0.928	0.947
0.55	0.704	0.807	0.857	0.885	0.907	0.919	0.937
0.5	0.692	0.796	0.846	0.874	0.896	0.908	0.926
0.45	0.678	0.783	0.834	0.861	0.883	0.895	0.913
0.4	0.662	0.769	0.820	0.847	0.868	0.881	0.898
0.35	0.643	0.753	0.804	0.831	0.851	0.865	0.882
0.3	0.621	0.733	0.785	0.812	0.832	0.846	0.862
0.25	0.595	0.709	0.762	0.789	0.809	0.823	0.838
0.2	0.562	0.680	0.733	0.762	0.780	0.795	0.809
0.15	0.519	0.639	0.694	0.725	0.743	0.759	0.771
0.1	0.458	0.579	0.636	0.669	0.689	0.706	0.717
0.05	0.353	0.471	0.530	0.566	0.589	0.607	0.618
Sample %	16	31	46	60	74	87	100

Canine Accuracy	Stratified (Skip Rows)				
	7	4	3	2	1
1	0.790	0.845	0.874	0.911	1.000
0.95	0.784	0.839	0.868	0.907	0.995
0.9	0.778	0.833	0.861	0.901	0.990
0.85	0.771	0.826	0.854	0.896	0.984
0.8	0.764	0.819	0.847	0.889	0.978
0.75	0.756	0.811	0.839	0.882	0.972
0.7	0.748	0.802	0.831	0.875	0.964
0.65	0.739	0.793	0.822	0.866	0.956
0.6	0.729	0.783	0.812	0.857	0.947
0.55	0.718	0.772	0.801	0.846	0.937
0.5	0.706	0.759	0.789	0.835	0.926
0.45	0.693	0.745	0.775	0.822	0.913
0.4	0.677	0.730	0.760	0.807	0.898
0.35	0.659	0.711	0.743	0.790	0.882
0.3	0.638	0.689	0.722	0.770	0.862
0.25	0.613	0.663	0.697	0.746	0.838
0.2	0.581	0.630	0.665	0.715	0.809
0.15	0.538	0.585	0.623	0.674	0.771
0.1	0.476	0.521	0.561	0.612	0.717
0.05	0.371	0.411	0.451	0.502	0.618
Sample %	22	29	36	50	100

For the simulation estimates, detection uncertainty = sampling uncertainty + canine detection accuracy. Highlighted are two groups of scenarios for 95% (red outline) and 75% (purple box) detection accuracy for canine perimeter surveys of 1 to 7 tree(s) depth and for stratified surveys of every 7th, 4th, 3rd, 2nd or single rows, respectively. Perimeter survey 7 trees deep and stratified survey of every (1) row, constitutes a complete census of all trees.

Movie Legends

Movie S1.

Canine 'Bello', a springer spaniel, interrogating citrus trees arranged in a 10 X 10 grid. Canine alerts by sitting next to the *C*Las-positive tree, i.e. target. This activity is repeated by re-randomizing locations of *C*Las-positive trees within the grid for both training and to test each canine for detection accuracy.

Movie S2.

Canine 'Zsemir', a Belgian malinois, interrogating metal cans containing non-infected and *C*Las-infected root samples. Canine alerts by sitting next to the can containing *C*Las-positive roots, i.e. target.

Movie S3.

Canine 'Mira', a German Shepard/Belgian malinois mix, interrogating citrus trees arranged in rows. Trees from the USDA, ARS Exotic Citrus Pathogen Collection in Beltsville, Maryland, USA placed on the lawn outside the facility. Canine alerts by sitting next to the *C*Las-positive tree, i.e. target but does not react to other citrus pathogens, incl. viruses, viroids, spiroplasma, and other bacteria. The canine continues the run of the remaining trees, incl. past two trees infected with *Sprioplasma citri* (causal agent of citrus stubborn) eventually coming to and alerting on a *C*Laf-positive tree, i.e. infected with *Candidatus* Liberibacter africanus, the African form of HLB.

Movie S4.

Canine 'Mira', a German Shepard/Belgian malinois mix, interrogating metal cans arranged in rows and each containing a small cage holding either non-infected or *C*Las-infected Asian citrus psyllid vectors. Canine alerts by sitting next to the can containing an insect cage with *C*Las-positive psyllids.

Movie S5.

Canine 'Maci', a Belgian malinois, interrogating red grapefruit trees in a commercial orchard in the Rio Grande Valley of Texas, USA. Canine runs along the row of trees and abruptly stops and sits 'alerts' when he acquires the scent profile of a *C*Las-positive tree. Note canine is wearing red rubber shoes to protect it from thorny weeds.

Movie S6.

Canine 'Szaboles', a Belgian malinois, interrogating citrus trees in a residential property in Los Angeles County, California, USA. Canine walks along the various plants located on the property. Here the canine interrogates a sable palm cycad in a pot, a potted lemon tree, and a *C*Las-positive orange tree. Canine stops and sits 'alerts' when he acquires the scent profile from the *C*Las-positive orange tree.

Movie S7.

Simulation of *C*Las epidemic over a 10-year period based on an SECIR model (see text). Simulation considers three disease control strategies of HLB i) canine, ii) PCR and iii) visual survey to detect *C*Las-infections. Commercial orchard size is 16.2 ha (40 ac) with < 1% initial infection occurring initially on the southern border and simulated survey is conducted on 180 day

intervals followed by removal of infected trees within 30 da post infection. Infected (I) class individuals are infectious and symptomatic whereas Cryptic (C) class individuals are infectious but asymptomatic. Comparisons of the three control strategies demonstrate improved orchard health and cost benefit of canine early detection. Corresponds to Fig. S21.

Movie S8.

Simulation of *C*Las epidemic over a 10-year period based on an SECIR model (see text). Simulation considers three disease control strategies of HLB i) canine, ii) PCR and iii) visual survey to detect *C*Las-infections. Commercial orchard size is 16.2 ha (40 ac) with < 1% initial infection occurring initially on the southern border and simulated survey is conducted on 180 day intervals followed by removal of infected trees within 30 da post infection. In this simulation cumulative tree removals over the prior year are replanted once per year in the first quarter. Infected (I) class individuals are infectious and symptomatic whereas Cryptic (C) class individuals are infectious but asymptomatic. Comparisons of the three control strategies demonstrate improved orchard health and cost benefit of canine early detection. Corresponds to Fig. S22.